Lawrence Berkeley Laboratory
UNIVERSITY OF CALIFORNIA

Materials & Molecular Research Division

BOUNDARY LAYER CONTROL BY MEANS OF STRONG INJECTION

Ruey-Jen Yang
(Ph.D. thesis)

February 1982

Prepared for the U.S. Department of Energy under Contract DE-AC03-76SF00098

DISCLAIMER

LBL-13807

BOUNDARY LAYER CONTROL BY MEANS OF STRONG INJECTION

Ruey-Jen Yang

Ph.D. Thesis

February 1982

Materials and Molecular Research Division
Lawrence Berkeley Laboratory
University of California
Berkeley, CA 94720

This work was supported by the Division of Material Sciences, Office of Basic Energy Sciences of the U.S. Department of Energy under Contract Number DE-AC03-76SF00098.

ACKNOWLEDGMENT

I wish to express my deepest gratitude to Professor Maurice Holt for his constant guidance and advice during my entire stay at Berkeley. Professor Holt's understanding and warm personality as well as his encouragement and wholehearted trust have won his students' highest respect.

Special thanks are extended to Dr. Alan Levy for his continued funding during the course of the research; to Professor W. S. Yeung and Professor C. A. J. Fletcher for their useful discussions on the numerical schemes; to Sheila Slavin for her skill in typing this manuscript; and to all my friends who shared a pleasant and fruitful life with me here.

Finally, I am grateful to my parents for their endless love; to my brother, Ruey-Chen, and my sisters, Sue-Wien and Chin-Yeir, for their warm affection.

This work was supported by the Division of Material Sciences, Office of Basic Energy Sciences, U.S. Department of Energy, through Contract Number DE-AC03-76SF00098.

LIST OF FIGURES

TABLE OF CONTENTS

BOUNDARY LAYER CONTROL BY MEANS OF STRONG INJECTION

by

Ruey-Jen Yang

ABSTRACT

The gas mixture produced by a coal gasifier contains components which have serious corrosive effects on the walls of the pipe flow system. To reduce these, a non-corrosive gas is injected into the stream of the coal gas products, in a direction parallel to the pipe wall. The interaction between the injected stream and the original pipe flow is investigated analytically and is an example of the so-called Wall Jet Problem.

The model adopted is that of a two-dimensional incompressible turbulent free mixing layer, with the corrosive gas H_2S forming the upper stream and moving faster than the injected non-corrosive gas in the lower stream, the latter bounded by the solid wall of the pipe. This wall jet flow can be divided into three distinct regions. In the first, farthest upstream, the upper (main) stream interacts with the lower injected stream in a free mixing process, while a turbulent boundary layer develops along the pipe wall bounding the lower stream. In the second region the lower half of the free mixing layer interacts with the wall turbulent boundary layer. In the third region, stream mixing has been completed and all diffusion takes place in a thickened turbulent boundary layer.

The orthonormal version of the numerical method of integral relations is applied to solve the momentum and species mean turbulent boundary layer equations, along with eddy viscosity modeling. Numerical results show that the ratio of the distance, where the mass concentration of H_2S diffuses to the wall surface to the slot height of injection, is of the order 0(100) for a given velocity ratio of two free streams in the mixing layer. The shear stress at the wall surface increases in the streamwise direction in the second region. This results from the larger momentum of the upper stream causing the sublayer of the wall boundary layer in the lower stream to become thinner.

Approved:

Maurice Holt 2.17.82

Maurice Holt, Chairman

I. INTRODUCTION

The current interest in energy conversion technology has focused attention on the production of synthetic natural gas from coal. Gas mixtures, in a coal gasification process, contain hydrogen, carbon dioxide, carbon monoxide, steam and hydrogen sulfide. Of those, hydrogen sulfide can cause very serious pipe corrosion. Furthermore, solid particles contained in the gas stream may be projected against a pipe wall causing erosion. In order to protect the pipe wall from attack by corrosive gas and damaging particles, an attempt is made to inject a non-corrosive fluid, at the pipe entry, to form a thin layer on the inner pipe wall. Thus the corrosive gas and solid particles can be "washed away" or "blown off" the wall for a time.

Mass injection into a turbulent boundary layer by tangential injection has been studied for many years. In the past decade, the practical applications of this technique include reduction of skin friction on an airfoil, prevention of boundary layer separation over a surface subject to adverse pressure gradient and protection of surface exposed to high-temperature environment encountered in combustion chambers, gas turbines, rocket nozzles, and high-speed flight vehicles. Recent works on this subject can be found in LaRue and Libby (1977, 1980), Cary, Bushnell and Hefner (1979) and Brune (1981). The flow condition at the initial stage considered by those authors is the confluent turbulent boundary layer forming when a turbulent flow above a splitter plate mixes with a fully developed turbulent channel flow beneath it.

In this work, we choose a simplified model shown in Fig. 1.

The first stream is assumed to be hydrogen sulfide, H_2S, the most corrosive component in the gas mixture from a coal gasifier. The second stream is the injected fluid, for example, steam. Both streams are assumed to be of uniform density and flow at constant low speeds. The flow is isothermal, two-dimensional, and the boundary layer effects on both sides of the splitter plate can be neglected. In other words, a model which is a two-dimensional incompressible turbulent free mixing layer in the presence of a wall is used in this analysis. A flow of this type involves the interaction of a free mixing layer and a wall boundary layer. Three zones can be physically perceived. Firstly, at the end of the splitter plate the upper and lower streams begin to mix; in the meantime, a wall boundary layer is developing along the wall. Also, before the two layers merge together, an embedded potential core exists in between. Recently, Pot (1979) conducted an experiment to observe the phenomena of the interaction between a turbulent wake and a turbulent wall layer. He found that the wake and the wall layer develop independently before the two layers merge. Therefore, in the present work, we assume that the free mixing layer and the wall layer are not to be influenced by each other in the first region. Secondly, just downstream of the position where these two layers merge, there is a domain within which the two viscous regions interact. Thus the mixing layer gradually dissolves into a new boundary layer type flow. Thirdly, far downstream from the origin of mixing, the stream mixing has been completed. In this zone the flow can be treated in terms of conventional turbulent boundary layer theory.

The purpose of this work is to find the location where the

concentration of the first stream diffuses to the wall. The species equation is decoupled from the momentum equation as a result of the assumption made, in which both streams are regarded as incompressible fluids with the same density, and are isothermal. Thus, the species equation can be solved separately after the momentum equation is solved.

The Method of Integral Relations (MIR), introduced by Dorodnitsyn (1960) provides a simple and accurate means of solving laminar boundary layer flows. No approximations are made to the equations. Approximations are made in representing unknown integrands appearing in the basic integral relations. In two-dimensional boundary layer flows, the approximation is based on the representation of the streamwise velocity gradient in the transverse direction as a simple algebraic function of the streamwise velocity itself. Such a representation should reflect the physical character of the flow. If polynomials are used, the order of the approximation depends on the degree of the polynomials. In principle this can be as high as desired, but in practice the order of approximation is limited by the inversion of the resulting matrix, which becomes progressively more ill-conditioned, and the amount of algebra required. However, these disadvantages have been largely overcome in the orthonormal version of MIR (Fletcher and Holt, 1975). As indicated by Yeung and Yang (1981), high order approximations should be used to solve turbulent boundary layer flows due to the highly inflected velocity profiles of the flows. We employ the orthonormal version of MIR in the present analysis.

This report is divided into three main parts. The first part discusses the numerical solution of the turbulent boundary layer flow and the orthonormal version of MIR is described in detail. The

numerical results are in very good agreement with experimental data. The second part discusses the numerical solution of the turbulent free mixing layer. Here MIR shows its advantage in that the approach yields a unique solution and this is independent of the third boundary condition (Ting, 1959). Comparisons between the numerical results and experimental data are also made. The third part discusses the numerical solution of the interaction between the turbulent wall layer and the turbulent free mixing layer. The location where the mass concentration of H_2S diffuses to the wall surface is found and some interesting physical phenomena are cited.

II. ANALYSIS OF THE TURBULENT WALL LAYER*

2.1 Introduction

In the vast body of literature dealing with turbulent boundary layer calculations, two major methods have been employed: the so-called integral method and the differential method. In this chapter, we investigate a particular solution procedure for the two-dimensional incompressible turbulent boundary layer using the Method of Integral Relations (MIR). In particular, the efficiency and versatility of this method, as applied to turbulent boundary layer calculations, is studied.

The method of integral relations has previously been applied to two-dimensional turbulent boundary layer calculations by Abbott and Deiwert (1968) and by Murphy and Rose (1968) at the 1968 Stanford Conference on turbulent boundary layer calculations. Unfortunately, that formulation was found to be inferior to other prediction methods presented at the same conference. Here, we shall reformulate the problem by using the modified version of MIR developed by Fletcher and Holt (1975). As a result, most of the shortcomings indicated by Murphy and Rose are overcome.

2.2 Formulation

For a two-dimensional, incompressible, steady flow, with the usual boundary layer approximations, the momentum and continuity equations, in terms of the time-averaged and fluctuating quantities, may be written in the form:

---

*Taken in part from the published paper by Yeung and Yang (1981).

$$u \frac{\partial u}{\partial x} + v \frac{du}{dy} = - \frac{1}{\rho} \frac{dp}{dx} + \frac{\partial}{\partial y} \left[(\nu + \frac{\varepsilon}{\rho}) \frac{\partial u}{\partial y} \right] \quad , \tag{2.1}$$

$$\frac{\partial u}{\partial x} + \frac{\partial v}{\partial y} = 0 \quad , \tag{2.2}$$

where u and v are the mean velocity components in the x and y directions, respectively, and p is the mean pressure; ρ is the density of the fluid and ν its kinematic viscosity. The eddy viscosity, ε, is defined as

$$- \rho \overline{u'v'} = \varepsilon \frac{\partial u}{\partial y} \quad , \tag{2.3}$$

where $- \rho \overline{u'v'}$ is the so-called Reynolds stress. The following non-dimensional variables are chosen:

$$U = \frac{u}{u_e} \quad , \quad V = \frac{vRe^{1/2}}{u_e} \quad , \quad \bar{x} = \frac{x}{L} \quad , \quad \bar{y} = \frac{yRe^{1/2}}{L} \quad , \quad U_e = \frac{u_e}{u_\infty} \quad , \tag{2.4}$$

where L and u_∞ are the characteristic length and velocity scales, respectively, u_e is the velocity at the outer boundary layer edge, and the Reynolds number Re is defined as

$$Re = \frac{u_\infty L}{\nu} \quad . \tag{2.5}$$

The pressure gradient is related to the outer edge velocity by Bernoulli's equation:

$$- \frac{1}{\rho} \frac{dp}{dx} = u_e \frac{du_e}{dx} \quad . \tag{2.6}$$

Using Eqs. (2.4) and (2.6), the original governing equations (2.1) and (2.2) become

$$U \frac{\partial U}{\partial \bar{x}} + V \frac{\partial U}{\partial \bar{y}} = \frac{1}{U_e} \frac{dU_e}{d\bar{x}} (1-U^2) + \frac{1}{U_e} \frac{\partial}{\partial \bar{y}} \left[(1 + \frac{\varepsilon}{\mu}) \frac{\partial U}{\partial \bar{y}} \right] \quad , \tag{2.7}$$

$$\frac{\partial U}{\partial \bar{x}} + \frac{\partial V}{\partial \bar{y}} = - \frac{U}{U_e} \frac{dU_e}{d\bar{x}} \tag{2.8}$$

To apply the Method of Integral Relations, we define a set of linearly independent functions $\{f_i(U)\}$ such that

$$f_i(1) = 0 \quad , \quad i = 1,2,\ldots,N \quad , \tag{2.9}$$

where N is the order of approximation. Multiply Eq. (2.8) by f_i and Eq. (2.7) by f_i', defined as the first derivative of f_i with respect to U, add and integrate from $\bar{y} = 0$ to $\bar{y} \to \infty$:

$$\frac{\partial}{\partial \bar{x}} \int_0^\infty f_i U d\bar{y} = \frac{1}{U_e} \frac{dU_e}{d\bar{x}} \int_0^\infty f_i'(1-U^2)\, d\bar{y} - \frac{1}{U_e} f_i'(0) \left(\frac{\partial U}{\partial \bar{y}}\right)_0$$

$$- \frac{1}{U_e} \int_0^\infty \left(1 + \frac{\varepsilon}{\mu}\right) \left(\frac{\partial U}{\partial \bar{y}}\right)^2 f_i'' d\bar{y} - \frac{1}{U_e} \frac{dU_e}{d\bar{x}} \int_0^\infty U f_i\, d\bar{y} \quad . \tag{2.10}$$

Change the variable of integration from $\bar{y}$ to U and define Z as:

$$Z = \left(\frac{\partial U}{\partial \bar{y}}\right)^{-1} \quad , \tag{2.11}$$

and Eq. (2.10) can be written as:

$$\frac{\partial}{\partial \bar{x}} \int_0^1 f_i U Z dU = \frac{1}{U_e} \frac{dU_e}{d\bar{x}} \int_0^1 \left[(1-U^2) f_i' - U f_i\right] Z dU$$

$$- \frac{1}{U_e} f_i'(0) \frac{1}{Z_o} - \frac{1}{U_e} \int_0^1 \left(1 + \frac{\varepsilon}{\mu}\right) \frac{f_i''}{Z} dU \quad . \tag{2.12}$$

Equation (2.12) is the basic integral relation in the present analysis.

We now further define $\{f_i\}$ as a set of orthonormal functions constructed from the Dorodnitsyn functions $(1-U)^k$, $k = 1,2,3\ldots$ by the Gram-Schmidt procedure (Isaacson and Keller, 1966). Hence:

$$f_i(U) = \sum_{k=1}^{i} c_{ik} (1-U)^k \quad , \tag{2.13}$$

and

$$\int_0^1 f_k f_j \frac{U}{1-U}\, dU = \delta_{kj} \quad , \tag{2.14}$$

with δ_{kj} being the Kronecker delta. Z is then represented by:

$$Z = \frac{b_o + \sum_{j=1}^{N-1} b_j f_j(U)}{1-U} \tag{2.15}$$

where $b_o, b_1, b_2, \ldots$ are unknown coefficients to be found. Substituting (2.15) into (2.12) and invoking (2.14), we obtain an explicit set of ordinary differential equations in the coefficients $b_o, b_1, \ldots, b_{N-1}$:

$$\frac{db_o}{d\bar{x}} \int_0^1 \frac{f_i U}{1-U}\, dU + \frac{db_i}{d\bar{x}} = \frac{1}{U_e}\frac{dU_e}{d\bar{x}} \int_0^1 [(1-U^2)f_i' - Uf_i] Z dU$$

$$- \frac{1}{U_e}\frac{f_i'(0)}{Z_o} - \frac{1}{U_e}\int_0^1 (1+\frac{\varepsilon}{\mu})\frac{f_i''}{Z}\, dU \quad ,$$

$$i = 1, 2, \ldots, N-1 \tag{2.16a}$$

and

$$\frac{db_o}{d\bar{x}} \int_0^1 \frac{f_N U}{1-U}\, dU = \frac{1}{U_e}\frac{dU_e}{d\bar{x}} \int_0^1 [(1-U^2)f_N' - Uf_N] Z dU$$

$$- \frac{1}{U_e} f_N'(0)\frac{1}{Z_o} - \frac{1}{U_e}\int_0^1 (1+\frac{\varepsilon}{\mu})\frac{1}{Z} f_N'' dU \quad , \tag{2.16b}$$

which can be integrated subject to appropriate initial conditions at some station $\bar{x} = \bar{x}_i$. We shall discuss the initial conditions later.

The above formulation is similar to that in a laminar boundary layer (Dorodnitsyn, 1960). Apart from the difficulty of evaluating the integral

$$\int_0^1 (1+\frac{\varepsilon}{\mu})\frac{1}{Z} f_i''(U) dU \quad ,$$

in which some kind of eddy viscosity model for ε has to be used, one problem is that the approximation of Z given by (2.15) is not accurate

unless N is rather large. This is mainly due to the highly inflected velocity profile in a turbulent boundary layer as opposed to the smooth profile in the laminar case. Thus, Murphy and Rose (1968) pointed out that the usual sequence $(1-U)^j$, $j = 1,2,...$ is not quite satisfactory, even when a four-parameter profile is used (i.e., $N = 4$). Instead, they judiciously assigned much larger exponents to the factor (1-U) and determined in the course of their numerical solution the optimum values of those exponents. This of course destroys the completeness requirement of the original method of integral relations, and it does not guarantee in principle that the approximation will converge to the exact solution if the order of approximation tends to infinity. The sole purpose of their scheme is apparently better to represent the Z profile in a turbulent boundary layer while using as few parameters as possible, since the traditional method of integral relations is quite impractical when too many parameters are used. However, the present orthonormal version circumvents this "high order" difficulty and enables one to preserve the completeness requirement while still using as many parameters as possible to represent faithfully the Z profile. Indeed, it has been applied to the two-dimensional laminar boundary layer to as high as $N = 15$ with little computer expense (Fletcher and Holt, 1975). It is therefore believed that the present formulation would be efficient even for large values of N.

2.2.1 Turbulence Modeling

In order to calculate the last integrals in Eqs. (2.16a) and (2.16b), a model for the eddy viscosity ε/μ is needed. We use the following expression for the wall region:

$$\frac{\varepsilon}{\mu} = 0.04432[e^{0.4u^+} - 1 - 0.4u^+ - 0.08u^{+2}] \quad , \tag{2.17}$$

which was first deduced by Spalding (1961) and later found independently by Kleinstein (1967). For the wake region, the Clauser model (1956) is used:

$$\frac{\varepsilon}{\mu} = 0.0168\ Re_{\delta*} \tag{2.18}$$

where $u^+ = u/u_\tau$ and $u_\tau = \sqrt{\tau_w/\rho}$, the wall frictional velocity. $Re_{\delta*}$ is defined as

$$Re_{\delta*} = \frac{u_e \delta^*}{\nu} \tag{2.19}$$

with δ^* being the usual displacement thickness.

The wall shear stress, τ_w, is given by:

$$\tau_w = (\mu+\varepsilon)_0 (\frac{\partial u}{\partial y})_0 \quad , \tag{2.20}$$

where the subscript 0 denotes the wall.

Experimental data show that the wall region extends to where the non-dimensional velocity U assumes a value of roughly 0.7 (Bradshaw, 1976, p. 53). In general, we denote this value by U_m. The determination of U_m will be discussed later. Hence the last integral in Eqs. (2.16a) and (2.16b) can be evaluated as

$$\int_0^1 (...)dU = \int_0^{U_m} (...)dU + \int_{U_m}^1 (...)dU \quad , \tag{2.21}$$

where (...) represents symbolically the integrand.

Before discussing the method used to calculate (2.21), we first derive expressions of u^+ and y^+ in terms of the present variables Z and U. We begin with Eq. (2.20):

$$\tau_w = (\mu + \varepsilon)_0 (\frac{\partial u}{\partial y})_0 \quad .$$

Since $\varepsilon = 0$ at $\bar{y} = 0$, we have:

$$\tau_w = \mu (\frac{\partial u}{\partial y})_0 \quad .$$

Using the definition of Z and the nondimensional variables defined in (2.4), it can be shown that

$$\frac{\tau_w \sqrt{Re}}{\rho u_\infty^2} = \frac{U_e}{Z_0}$$

or

$$\left(\frac{u_\tau}{u_\infty}\right)^2 = \frac{U_e}{Z_0 Re^{\frac{1}{2}}} \quad . \tag{2.22}$$

Hence,

$$u^+ = U \sqrt{U_e Z_0 Re^{\frac{1}{2}}} \tag{2.23}$$

and

$$y^+ = \sqrt{\frac{U_e Re^{\frac{1}{2}}}{Z_0}} \quad \bar{y} \quad . \tag{2.24}$$

Thus the eddy viscosity can be written in terms of Z and U as follows:

For $0 \leqslant U < U_m$

$$\frac{\varepsilon}{\mu} = 0.04432 \left[e^{0.4U \sqrt{U_e Z_0 Re^{\frac{1}{2}}}} - 1 - 0.4U \sqrt{U_e Z_0 Re^{\frac{1}{2}}} - 0.08 U^2 U_e Re^{\frac{1}{2}} Z_0 \right] , \tag{2.25}$$

and for $U_m \leqslant U \leqslant 1$

$$\frac{\varepsilon}{\mu} = 0.0168 \; U_e Re^{\frac{1}{2}} \int_0^1 (1-U) Z dU \tag{2.26}$$

and the displacement thickness δ^* has been written as

$$\delta^* = \int_0^\delta (1 - \frac{u}{u_e}) dy = \frac{L}{Re^{\frac{1}{2}}} \int_0^1 (1-U) Z dU \quad . \tag{2.27}$$

2.2.2 Evaluation of Integrals

The integrals in Eqs. (2.16a) and (2.16b) can be computed exactly except for the shear integrals, which appear as the last term in the equations. At present, these shear integrals are evaluated by using a method based on the Gaussian-Legendre rule, the algorithm of which is available in the Sandia Mathematical Library.

2.2.3 Determination of U_m

Up to now, we have only denoted the outer boundary of the wall region by U_m. As mentioned before, experimental results indicate that U_m is roughly 0.7. However, this value of U_m may not produce a continuous curve for ε/μ across the whole boundary layer. To be consistent with the present formulation, then, U_m must be found by determining the intersection of the ε/μ in the inner region with that in the outer region. Hence, equating the two expressions (2.25) and (2.26), we have:

$$0.04432\left[e^{0.4U\sqrt{U_e Z_0 Re^{\frac{1}{2}}}} - 1 - 0.4U\sqrt{U_e Z_0 Re^{\frac{1}{2}}} - 0.08U^2 U_e Z_0 Re^{\frac{1}{2}}\right]$$

$$= 0.0168 U_e Re^{\frac{1}{2}} \int_0^1 (1-U) Z dU \quad . \tag{2.28}$$

The above equation can be solved iteratively to yield U_m. The advantage of using Spalding's model becomes clear: this model is explicit in U and hence makes it easier to determine U_m. The solution is sought in the neighborhood of 0.7. In the case of flow with adverse pressure gradient, the wake region becomes substantial and U_m is found to be smaller than that of the flow with favorable pressure gradient or without pressure gradient. Once U_m is determined, the shear integrals can be evaluated as mentioned earlier.

2.2.4 Initial Conditions

The system of ordinary differential equations (ODE) resulting from our formulation of the MIR must be provided with initial conditions on the parameters b_o and b_j at some initial station, which can be taken as zero by suitable translation of the origin. Unlike laminar boundary layer flows, where the initial conditions are usually given by exact solutions (similarity solution), we have to rely on experimental data to determine the appropriate initial conditions. The easiest way in the present formulation is to calculate these initial values from experimental data. In general, among the experimental data, velocity profile U, boundary layer thickness δ, displacement thickness δ^*, momentum thickness θ, and skin-friction coefficient C_f are available. One then faces the problem of choosing the most "effective" data. Our suggestion on these choices is as follows:

(a) The skin-friction coefficient, C_f, is the most effective for ensuring the correct behavior of the velocity profile at the wall.

(b) Second in effectiveness is δ, the boundary layer thickness. Although Eq. (2.15) satisfies the boundary conditions $\partial U/\partial \bar{y} \to 0$ automatically as $\bar{y} \to \infty$, the value of the boundary layer thickness would not generally match the experimental data. Hence, to match the boundary layer thickness is to secure a more correct boundary condition at the outer edge of the layer.

(c) Displacement thickness, δ^*, is our third choice of data. In (a) and (b), we specify the boundary conditions at the wall and at the outer edge of the layer. By matching the

displacement thickness, we expect to get a correct global behavior of the velocity profile in the boundary layer.

It was found that using the above three conditions (i.e., C_f, δ, δ^*, for N = 3) to compute the flow over a flat plate, a very satisfactory result was obtained. In the case of higher approximations, more data are needed. Generally, a trial-and-error procedure is needed to choose other "effective" data. However, one can pinpoint these data after several attempts by noting that good initial conditions should behave as $|b_0| > |b_1| > |b_2| \ldots$ in Eq. (2.15). Since U = 0 at the wall, Eq. (2.15) becomes:

$$Z_0 = b_0 + \sum_{j=1}^{N-1} b_j f_j(0) = b_0 + \sum_{j=1}^{N-1} b_j \left(\sum_{k=1}^{j} c_{jk} \right) \quad . \tag{2.29}$$

In the course of constructing orthonormal functions from $(1-U)^k$ by the Gram-Schmidt procedure, we found that

$$\left| \sum_{k=1}^{j-1} c_{jk} \right| < \left| \sum_{k=1}^{j} c_{jk} \right| \quad .$$

Intuitively, the contribution to Z from the subsequent term in Eq. (2.29) should become smaller as the order of approximation gets higher. Therefore, as noted, we expect that good initial conditions should yield $|b_0| > |b_1| > |b_2| > \ldots$[†]

2.3 Results and Discussion

Flow with zero pressure gradient is tested by the present formulation. Flows with favorable and adverse pressure gradient were reported by Yeung and Yang (1981). The properties of the fluid are chosen to be identical to those given by Cole and Hirst (1968)

[†] In our calculations, however, this condition was not always met.

for the case ID 1400. Figures 2 to 6 show comparisons between the predicted and measured values of the various flow quantities. Surprisingly good results were obtained with the approximation N = 3 just by using the initial conditions that matched C_f,δ and δ^*. This supports the "effectiveness" of the data C_f,δ and δ^* in the determination of initial conditions. The computer time of this approximation is about 5 sec in a CDC-7600 machine. Results of the approximations for N = 4 and N = 5 also show excellent agreement with measured values.

It should be pointed out that the CPU time for N = 5 (45 sec) is much greater than that for N = 4 (8 sec). This is due to the stiffness of the system of ODE's in Eqs. (2.16a) and (2.16b), in which the coefficients of c_{ik} in Eq. (2.13) get larger as N increases. Nevertheless, the CPU times for the present formulation are smaller than those quoted in Murphy and Rose (1968), taking into consideration the different computers used.

III. ANALYSIS OF THE TURBULENT FREE MIXING LAYER

3.1 Introduction

The characteristics of a turbulent mixing layer initiated by the confluence of two parallel streams has been of interest for many years because of its broad applications in technology. Early studies of this subject were made by Tollmien (1926), Kuethe (1935) and Görtler (1942). These classical solutions of the problem are based on the assumptions that the change of velocity from that of one stream to the other takes place in a mixing region of small thickness compared to the length of mixing in the streamwise direction and that the normal component of the velocity, v, is small compared to the component of velocity parallel to the main stream, u. Moreover, all of the solutions except that of Kuethe are based on an arbitrary third boundary condition (Ting, 1959).

Within the framework of boundary layer theory, the solution is unique for a flow over a plate by specifying three conditions, namely at $y = 0$ (i.e., on the plate surface) $u = v = 0$, and at $y \to \infty$, $u \to u_\infty$ (∞ denotes free stream condition). However, the solution is nonunique for the mixing problem since only two conditions are available, namely $u \to U_1$ as $y \to \infty$, and $u \to U_2$ as $y \to -\infty$. The absence of a third boundary condition admits an infinite number of solutions to the mixing problem. Mathematically, if $g(y)$ is a solution satisfying the boundary conditions at $y = \pm\infty$, so is $g(y+c)$, where c is any constant. It is known that to compare this solution with experimental data, the theoretical distribution of axial velocity must be shifted in the transverse direction, so as to obtain a better

agreement with experimental data.

Tollmien (1926) obtained an analytical solution for the mean velocity profile of a mixing layer with the lower stream at rest (i.e., $U_2 = 0$) by applying Prandtl's mixing length hypothesis for the turbulent shear stress. He fixed his solution by making the transverse velocity v_1 vanish at the outer edge $y \to \infty$. Kuethe (1935) extended Tollmien's approach to the case of two non-zero velocity streams, using von Karman's suggestion that the third boundary condition should correspond to no external forces acting on the total fluid system perpendicular to the main flow, i.e., $U_1 v_1 + U_2 v_2 = 0$. However, the proof is not convincing. Later, Görtler (1942) solved the same problem as Kuethe by using Prandtl's second hypothesis for the turbulent shear stress (i.e., the constant eddy viscosity hypothesis). He avoided the question of the third boundary condition. Instead, he fixed his solution by saying that the mean speed $(U_1 + U_2)/2$ of the stream is along the line $y = 0$. In addition, he introduced an empirical constant related to the rate of spread of the mixing layer and to the free stream velocity ratio. Mills (1968) noticed that the governing equations for the mixing problem, written in terms of Crocco variables, no longer contain the variable v, for which the boundary condition is not sufficient, and hence the problem has a unique solution. The unique solution is independent of the form of the third boundary condition.

The Method of Integral Relations (MIR) originally developed by Dorodnitsyn (1960), and later modified by Fletcher and Holt (1975), has been applied successfully by Yeung and Yang (1981) to calculate the two-dimensional incompressible turbulent boundary layer. In this chapter, we discuss the application of MIR to the turbulent plane mixing

problem. Similar to Mills' formulation, MIR renders the governing equations for mixing problems in a form containing no v by judiciously selecting a set of weighting functions. Thus, a unique solution exists and is independent of the third boundary condition. Unlike Mills' method which needs successive approximation, after using a transformation to weaken the singularity at the outer edges of the mixing layer, the present method overcomes the singularity by appropriate weighting functions.

3.2 Formulation

It was observed by Brown and Roshko (1974) that density effects on the spreading angle of turbulent plane mixing between two streams of different gases were relatively small; the strong effects were due to compressibility. Thus a turbulent mixing of two semi-infinite streams of a homogeneous incompressible fluid, shed from a splitter plate, is assumed for the present study. It is well known that the contribution of molecular transport in all equations governing a fully developed free turbulent mixing of two streams at larger Reynolds number can be neglected. With this information the usual time-averaging techniques and assumptions associated with the boundary layer approximation of the mixing process lead, for two-dimensional, isobaric, steady flow, to the equations:

$$\frac{\partial u}{\partial x} + \frac{\partial v}{\partial y} = 0 \quad , \tag{3.1}$$

$$u \frac{\partial u}{\partial x} + v \frac{\partial u}{\partial y} = \frac{\partial}{\partial y} \left(\nu_t \frac{\partial u}{\partial y} \right) \quad , \tag{3.2}$$

$$u \frac{\partial m}{\partial x} + v \frac{\partial m}{\partial y} = \frac{\partial}{\partial y} \left(D_t \frac{\partial m}{\partial y} \right) \quad , \tag{3.3}$$

where u and v are the mean velocity components in the x and y directions, respectively; the origin is taken as the point at which mixing begins; m is the mean mass concentration of the upper stream, and ν_t and D_t are defined, in analogy with molecular diffusion, as

$$- \overline{u'v'} = \nu_t \, \partial u/\partial y \quad , \tag{3.4}$$

$$- \overline{m'v'} = D_t \, \partial m/\partial y \quad , \tag{3.5}$$

where u',v' and m' are fluctuating quantities. The coefficients ν_t and D_t need empirical relations which will be discussed later. The boundary conditions for Eqs. (3.1), (3.2) and (3.3) are

$$y \to \infty \quad , \quad u \to U_1 \quad , \quad m \to M_1 \quad ,$$

$$y \to -\infty \quad , \quad u \to U_2 \quad , \quad m \to 0 \quad .$$

It is convenient to work with the following non-dimensional variables:

$$\begin{aligned} U &= (u - U_2)/(U_1 - U_2) \quad , \quad \lambda = U_2/U_1 \quad , \\ V &= (v - U_2)/(U_1 - U_2) \quad , \quad M = m/M_1 \quad . \end{aligned} \tag{3.6}$$

Using (3.6), the governing equations (3.1), (3.2), (3.3) and the corresponding boundary conditions become

$$\frac{\partial U}{\partial x} + \frac{\partial V}{\partial y} = 0 \quad , \tag{3.7}$$

$$\left(U + \frac{\lambda}{1-\lambda}\right) \frac{\partial U}{\partial x} + \left(V + \frac{\lambda}{1-\lambda}\right) \frac{\partial U}{\partial y} = \frac{1}{U_1 - U_2} \frac{\partial}{\partial y} \left(\nu_t \frac{\partial U}{\partial y}\right) \quad , \tag{3.8}$$

$$\left(U + \frac{\lambda}{1-\lambda}\right) \frac{\partial M}{\partial x} + \left(V + \frac{\lambda}{1-\lambda}\right) \frac{\partial M}{\partial y} = \frac{1}{U_1 - U_2} \frac{\partial}{\partial y} \left(D_t \frac{\partial M}{\partial y}\right) \quad , \tag{3.9}$$

$$y \to \infty \quad , \quad U \to 1 \quad , \quad M \to 1 \quad ,$$

$$y \to -\infty \quad , \quad U \to 0 \quad , \quad M \to 0 \quad . \tag{3.10}$$

Using the assumptions $\nu_t = D_t$ and M is a function of U only, one can easily show that M = U from Eqs. (3.8), (3.9) and (3.10). Although the spread of species concentration is not the same as that of momentum in the turbulent mixing problem, the above assumptions are not bad for the short distance in which we are interested along the streamwise direction. This is because the boundary layer thickness grows linearly with respect to x, as is well known in the literature (see for example, Townsend, 1976). Therefore, once the velocity profile has been determined, the species concentration profile can also be obtained through M = U.

Let $\{f_i(U)\}$ be a set of linearly independent functions which satisfy $f_i(0) = f_i(1) = 0$, where $i = 1,2,\ldots,N$, and N denotes the order of approximation. Multiply Eq. (3.7) by f_i and Eq. (3.8) by f_i', defined as the first derivative of f_i with respect to U, add and integrate from $y \to -\infty$ to $y \to \infty$:

$$\frac{\partial}{\partial x} \int_{-\infty}^{\infty} f_i (U + \frac{\lambda}{1-\lambda}) dy = \frac{-1}{U_1 - U_2} \int_{-\infty}^{\infty} \nu_t f_i'' (\frac{\partial U}{\partial y})^2 dy \quad . \tag{3.11}$$

Change the variable of integration from y to U and define Z as

$$Z = (\frac{\partial U}{\partial y})^{-1} \quad .$$

Then, Eq. (3.11) can be written as

$$\frac{\partial}{\partial x} \int_0^1 f_i (U + \frac{\lambda}{1-\lambda}) Z dU = \frac{-1}{U_1 - U_2} \int_0^1 \nu_t f_i'' \frac{1}{Z} dU \quad . \tag{3.12}$$

Notice that the above equation is exact since we have not made any assumption for V at $y = \pm\infty$. V is cancelled through $f_i(0) = f_i(1) = 0$.

Since V no longer appears in the present formulation, the traditional third boundary condition for the mixing problem does not exist.

Z has a singularity of the following type:

$$Z \sim \frac{1}{U(1-U)}$$

due to the behavior of velocity profile at both edges of the mixing layer, i.e., 1/Z approaches zero as $U \to 0$ and $U \to 1$. In order to make the integral on the right-hand side of Eq. (3.12) finite, the functions f_i are chosen as $U^k(1-U)^k$ or the combination of $U^k(1-U)^k$, $k = 1,2,\ldots$ This is consistent with the conditions which we impoased on f_i before, i.e., $f_i(0) = f_i(1) = 0$.

To apply the orthonormal version of MIR, we represent

$$Z(U + \frac{\lambda}{1-\lambda}) = \frac{a_o + \sum_{j=1}^{N-1} a_j f_j}{U(1-U)} \quad , \tag{3.13}$$

where $a_o, a_1, \ldots, a_{N-1}$ are unknown coefficients to be found, and $\{f_i\}$ is a set of orthonormal functions constructed from $U^k(1-U)^k$ by the Gram-Schmidt procedure (Isaacson and Keller, 1966). Hence:

$$f_i(U) = \sum_{k=1}^{i} d_{ik} U^k (1-U)^k$$

and

$$\int_0^1 f_i f_j \frac{dU}{U(1-U)} = \delta_{ij} \quad . \tag{3.14}$$

with δ_{ij} being the Kronecker delta. Substituting Eq. (3.13) into Eq. (3.12) and invoking Eq. (3.14), we obtain an explicit set of ordinary differential equations in the coefficients $a_o, a_1, \ldots, a_{N-1}$:

$$\frac{da_o}{dx}\int_0^1 \frac{f_i}{U(1-U)}\,dU + \frac{da_i}{dx} = \frac{-1}{U_1-U_2}\int_0^1 \nu_t f_i''\,\frac{dU}{Z} \quad ,$$

$$i = 1,2,\ldots,N-1 \qquad (3.15)$$

and

$$\frac{da_o}{dx}\int_0^1 \frac{f_N}{U(1-U)}\,dU = \frac{-1}{U_1-U_2}\int_0^1 \nu_t f_N''\,\frac{dU}{Z} \quad , \qquad (3.16)$$

which can be integrated subject to appropriate initial conditions at some station $x = x_i$. We shall discuss the initial conditions later.

3.2.1 Turbulence Modeling

Prandtl (1942) proposed a model, Eq. (3.4), which is analogous to the Newtonian law of friction in laminar flow. He assumed that the coefficient of turbulent viscosity, ν_t, is constant over a cross section of the free mixing layer. He obtained

$$\nu_t = \kappa\delta(U_1-U_2) \quad , \qquad (3.17)$$

where δ is the width of the mixing zone; κ is an empirical constant which is equal to 0.0044. In terms of the present variables Z and U, Eq. (3.17) becomes

$$\nu_t = \kappa(U_1-U_2)\int_0^1 Z\,dU \quad . \qquad (3.18)$$

It is clear that ν_t is a function of x only.

3.2.2 Location of the Dividing Streamline

Using Eqs. (3.1) and (3.2), and noting that the transverse velocity component v is zero while the tangential shear stress is continuous along the dividing streamline, one can obtain:

$$\int_0^\infty u(U_1-u)\,dy + \int_{-\infty}^0 u(U_2-u)\,dy = 0 \quad .$$

Here the dividing streamline is chosen as the x-axis passing through the origin. Denote U_d as the dimensionless velocity component along the x-axis and use the present variables U and Z. Then the above relation becomes:

$$\int_{U_d}^{1} UZdU + \frac{\lambda}{1-\lambda}\int_{U_d}^{1} ZdU = \int_{0}^{1} U^2ZdU + \frac{\lambda}{1-\lambda}\int_{0}^{1} UZdU \quad . \tag{3.19}$$

An iteration procedure has to be used to obtain U_d which is a function of x. Once U_d is found, the location y can be calculated from the following relation:

$$y = \int_{U_d}^{U} ZdU \quad . \tag{3.20}$$

3.2.3 Initial Conditions

Initial values of $\{a_o, a_1, \ldots, a_{N-1}\}$ at an initial station x_i, have to be specified in order to integrate the system of ordinary differential equations (3.15) and (3.16). It may be deduced from the momentum equation that a turbulent mixing layer between two constant velocity incompressible free streams can be self-preserving (see for example, Townsend, 1976). Thus, the initial condition can be selected fairly arbitrarily, say from experimental data or from the approximate analytical solutions, provided that they do not contradict boundary conditions at $y = \pm\infty$ when the self-preserving solution is of interest.

Görtler's solution gives a good approximation to the shape of the observed mean velocity profile, although it has to be shifted bodily in the transverse direction in order to fit the experimental data. However, this shift is independent of the slope, $\partial U/\partial y$, of the mean velocity profile for a given U value. Here Görtler's solution

is illustrated to obtain the necessary conditions. Görtler's solution gives

$$U = \tfrac{1}{2}(1 + \frac{2}{\sqrt{\pi}} \int_0^{\xi} e^{-q^2} dq) \quad , \quad \xi = \sigma y/x \quad , \tag{3.21}$$

where σ is a constant which has the following empirical relation (Birch and Eggers, 1972):

$$\sigma = \frac{\sigma_o(1+\lambda)}{1-\lambda} \quad , \quad \sigma_o = 11 \quad .$$

Thus, the slope of U gives

$$\frac{1}{Z} = \frac{\partial U}{\partial y} = \frac{1}{\sqrt{\pi}} \frac{\sigma}{x} e^{-\xi^2} \quad . \tag{3.22}$$

Comparing Eqs. (3.13) and (3.22), and invoking Eq. (3.21), we obtain N coupled algebraic equations in N unknowns, $a_o, a_1, \ldots, a_{N-1}$. Thus, solution for the N unknowns can be found, for example, by an iteration procedure.

3.3 Results and Discussion

With λ being a parameter, several cases were tested using the 4th approximation (N = 4) and results are shown in Figs. 7 and 8. A recent review on the experimental data of turbulent plane mixing layer has been completed by Rodi (1975). Experimental data were marked on the same figures whenever appropriate. Figure 7 shows that the mixing layer penetrates more into the lower-speed stream than it does into the higher-speed stream. This is due to the continual deceleration of the fluid on the higher-speed side of the mixing layer and the acceleration of the fluid on the lower-speed side, which results in a slight deflection of the streamlines towards the lower-speed stream. In addition, lines of constant velocity ratio

show the linear dependence on distance in the streamwise direction. This can also be seen from similarity analysis and is confirmed by all experimental data.

A comparison of the mean velocity distribution at the different longitudinal positions shows that the mixing layers have a region in which geometric similarity exists and in this region the mixing layer is self-preserving. Figure 8 shows the U profiles against $y^* = (y-y_{0.5})/(y_{0.1}-y_{0.9})$, where $y_{0.5}$ refers to the value of y at $U = 0.5$, others likewise. The agreement between the theoretical and experimental results is seen to be quite good. We observe that there is almost no change in the shape of the mean velocity profile with respect to the velocity ratio except at the edge of low U. This change in shape is also observed in experiments. In addition, it was shown from numerical experiments that U profiles against y^* do not depend on κ, the empirical constant for turbulent viscosity ν_t. Thus, the numerical values of κ can be selected arbitrarily if one wants to find the self-preserving solution of the problem.

IV. ANALYSIS OF THE INTERACTION BETWEEN THE FREE MIXING LAYER AND THE WALL LAYER

4.1 Formulation

The turbulent free mixing layer merges with the turbulent wall layer at $x = x_o$ (see Fig. 1) and the interaction between these two layers then begins. The velocity distribution at, and the location of, station x_o can be obtained from Chapters 2 and 3 by the assumption that the free mixing layer and the wall layer develop independently in the x-direction and the velocity distribution of the merged flow at x_o is simply the linear superposition of the mean velocity profiles of the two layers. The justification for this assumption is presented in Pot (1979). We assume that the boundary layer approximations still apply to the merged flow. Therefore, the problem to be considered here may be formulated as follows: At a given station $x = x_o$, the velocity profile is known; determine the downstream development of the boundary layer with this initial profile.

The governing equations for the mean quantities of the merged flow, which is still assumed to be two-dimensional, isobaric and incompressible, are:

$$\frac{\partial u}{\partial x} + \frac{\partial v}{\partial y} = 0 \quad , \tag{4.1}$$

$$u \frac{\partial u}{\partial x} + v \frac{\partial u}{\partial y} = \frac{\partial}{\partial y} \left[\left(\nu + \frac{\varepsilon}{\rho} \right) \frac{\partial u}{\partial y} \right] \quad , \tag{4.2}$$

$$u \frac{\partial m}{\partial x} + v \frac{\partial m}{\partial y} = \frac{\partial}{\partial y} \left[(D + D_t) \frac{\partial m}{\partial y} \right] \quad , \tag{4.3}$$

where u and v are the mean velocity components in the x and y directions, respectively; m is the mean mass concentration of the upper stream; ρ is the density, ν is the kinematic viscosity, and D is the coefficient of mass diffusivity of the merged fluid flow. The quantities ε/ρ and D_t are defined as

$$\nu_t = \varepsilon/\rho = -\overline{u'v'}/\frac{\partial u}{\partial y} \quad , \tag{4.4}$$

$$D_t = -\overline{m'v'}/\frac{\partial m}{\partial y} \quad , \tag{4.5}$$

where u',v' and m' are fluctuating quantities. The modeling for ε/ρ and D_t will be discussed later. The boundary conditions are

$$y = 0 \quad , \quad u = 0 \quad , \quad v = 0 \quad , \quad \partial m/\partial y = 0 \quad ,$$

$$y \to \infty \quad , \quad u \to U_1 \quad , \quad m \to M_1 \quad ,$$

where the subscript 1 denotes the free stream condition which is constant. Introduce the following nondimensional variables:

$$U = \frac{u}{U_1} \quad , \quad V = \frac{vRe^{\frac{1}{2}}}{U_1} \quad , \quad \bar{x} = \frac{x}{L} \quad ,$$

$$\bar{y} = \frac{yRe^{\frac{1}{2}}}{L} \quad , \quad M = \frac{m}{M_1} \quad , \quad Re = \frac{U_1 L}{\nu} \quad . \tag{4.6}$$

Here L is a reference length. Using Eq. (4.6), the governing equations and the corresponding boundary conditions become:

$$\frac{\partial U}{\partial \bar{x}} + \frac{\partial V}{\partial \bar{y}} = 0 \quad , \tag{4.7}$$

$$U\frac{\partial U}{\partial \bar{x}} + V\frac{\partial U}{\partial \bar{y}} = \frac{\partial}{\partial \bar{y}}\left[\left(1 + \frac{\varepsilon}{\rho}\right)\frac{\partial U}{\partial \bar{y}}\right] \quad , \tag{4.8}$$

$$U \frac{\partial M}{\partial \bar{x}} + V \frac{\partial M}{\partial \bar{y}} = \frac{\partial}{\partial \bar{y}} \left[\left(\frac{D}{\nu} + \frac{D_t}{\nu_t} \frac{\varepsilon}{\mu} \right) \frac{\partial M}{\partial \bar{y}} \right] \quad , \tag{4.9}$$

$$\begin{gathered} \bar{y} = 0 \quad , \quad U = V = 0 \quad , \quad \partial M / \partial \bar{y} = 0 \quad , \\ \bar{y} \to \infty \quad , \quad U \to 1 \quad , \quad M \to 1 \quad . \end{gathered} \tag{4.10}$$

Notice that the species equation is decoupled from the momentum equation. Therefore, the species equation can be solved separately after the momentum equation. To solve the momentum equations by means of MIR, which has been described in Chapter 2, we have the following basic integral relation:

$$\frac{\partial}{\partial \bar{x}} \int_0^1 f_i U Z dU = - \frac{f_i'(0)}{Z_o} - \int_0^1 \left(1 + \frac{\varepsilon}{\mu} \right) \frac{f_i''}{Z} dU \quad , \tag{4.11}$$

where the weighting function $f_i(U)$ and the definition of Z are given in Eqs. (2.9) and (2.11), respectively. We also assume M is a function of U only. Multiplying Eqs. (4.7), (4.8) and (4.9) by $f_i M, f_i' M$ and f_i, respectively, adding and then integrating the result across the boundary layer with respect to $\bar{y}$, and introducing the variable Z, we get the basic integral relation for the mass concentration which reads

$$\begin{aligned} \frac{\partial}{\partial \bar{x}} \int_0^1 f_i U M Z dU = & - \frac{M_o f_i'(0)}{Z_o} - \int_0^1 \left[1 + \frac{D}{\nu} + \left(1 + \frac{D_t}{\nu_t} \right) \frac{\varepsilon}{\mu} \right] \frac{f_i'}{Z} \frac{dM}{dU} dU \\ & - \int_0^1 \left(1 + \frac{\varepsilon}{\mu} \right) M \frac{f_i''}{Z} dU \quad . \end{aligned} \tag{4.12}$$

The above equation can be further simplified by noting that for $U < U_o$, where U_o is the streamwise velocity component at the lower edge of the concentration boundary layer, M is equal to zero. Thus, before the concentration of the first stream diffuses to the wall surface,

Eq. (4.12) is reduced to

$$\frac{\partial}{\partial \bar{x}} \int_{U_o}^{1} f_i UMZ\,dU = -\int_{U_o}^{1} \left[1 + \frac{D}{\nu} + \left(1 + \frac{D_t}{\nu_t}\right) \frac{\varepsilon}{\mu}\right] \frac{f_i'}{Z} \frac{dM}{dU}\, dU$$

$$- \int_{U_o}^{1} \left(1 + \frac{\varepsilon}{\mu}\right) M \frac{f_i''}{Z}\, dU \quad . \tag{4.13}$$

Notice that U_o is a function of x, it is equal to U_2/U_1 at $x = x_o$ where the free mixing layer merges with the wall layer and equal to zero at the wall surface, where the concentration of the upper stream diffuses.

The interpolating function for Z is chosen from Eq. (2.15) and weighting functions for f_i are given by Eq. (2.13), satisfying Eq. (2.14). The interpolating function for M is chosen to satisfy its physical boundary conditions, namely at $U = 1$, $M = 1$; and at $U = U_o$, $\partial M/\partial \bar{y} = 0$, $M = 0$. To the first approximation,

$$M = \left(\frac{U - U_o}{1 - U_o}\right)^2 \quad . \tag{4.14}$$

Substituting expressions of Z, f_i and M in Eqs. (4.11) and (4.13), we obtain a system of ordinary differential equations:

$$\frac{db_o}{d\bar{x}} \int_0^1 \frac{f_i U}{1-U}\, dU + \frac{db_i}{d\bar{x}} = -\frac{f_i'(0)}{Z_o} - \int_0^1 \left(1 + \frac{\varepsilon}{\mu}\right) \frac{f_i''}{Z}\, dU \quad ,$$

$$i = 1,2,\ldots,N-1 \quad , \tag{4.15a}$$

$$\frac{db_o}{d\bar{x}} \int_0^1 \frac{f_N U}{1-U}\, dU = -\frac{f_N'(0)}{Z_o} - \int_0^1 \left(1 + \frac{\varepsilon}{\mu}\right) \frac{f_N''}{Z}\, dU \quad , \tag{4.15b}$$

and

$$A_1 \frac{dU_o}{d\bar{x}} + A_2 \frac{db_o}{d\bar{x}} + A_3 \frac{db_1}{d\bar{x}} + \cdots + A_{N+1} \frac{db_{N-1}}{d\bar{x}}$$

$$= -\int_{U_o}^{1} \left[1 + \frac{D}{\nu} + \left(1 + \frac{D_t}{\nu_t}\right) \frac{\varepsilon}{\mu}\right] \frac{f_1'}{Z} \frac{dM}{dU}\, dU \quad , \tag{4.16}$$

where $A_1, A_2, \ldots, A_{N+1}$ are certain coefficients varying with N. For example, if we choose N = 3 then

$$A_1 = -b_o(1 + U_o)/6 + (3U_o^2 - U_o - 2)(b_1c_{11} + b_2c_{21})/30$$
$$- b_2c_{22}(1 - 3U_o^2 + 2U_o^3)/30 \quad ,$$

$$A_2 = (3 - 2U_o - U_o^2)/12 \quad ,$$

$$A_3 = c_{11}(3 - 4U_o - U_o^2 + 2U_o^3)/60$$

$$A_4 = c_{11}(3 - 4U_o - U_o^2 + 2U_o^3)/60$$
$$+ c_{22}(1 - 2U_o + 2U_o^3 - U_o^4)/60 \quad .$$

Initial conditions for the system of the ordinary differential equations (4.15) and (4.16) are discussed later.

4.1.1 Turbulence Modeling

Pot (1979) conducted an experiment to investigate the behavior of the interaction between a wake and a wall layer. He found that the flow was not that of a normal equilibrium boundary layer during the interaction process. However, many problems have been solved in the literature by employing the traditional Prandtl's mixing length concept and Van Driest-Clauser eddy viscosity model to predict the same type of flow (Cary, Bushnell and Hefner, 1979; Miner and Lewis, 1974; Dvorak, 1973; Kacker, Pai and Whitelaw, 1969). Reasonable results, in comparison with experimental data, were obtained.

The turbulence structure of the interaction between the free mixing layer and the wall layer is complex and so far little understood. Seban and Back (1962) correlated the experimental data for

the mean velocity profile in turbulent boundary layers with tangential injection. They found that the mean velocity distribution was in good correspondence with the law of the wall and the law of the wake if the initial boundary layer effects on the splitter plate at the slot was thin. Hence we have confidence to employ the models, Eqs. (2.17) and (2.18), resulting from the law of the wall and the law of the wake to predict the type of flow considered herein since the effects of the initial boundary layer on both sides of the splitter plate are assumed to be negligible.

The magnitude of the turbulent mass diffusivity, D_t, is always of the same order of magnitude as the turbulent eddy viscosity, ν_t (Bradshaw 1976, p. 233). Experimental values of the turbulent Schmidt number $S_{ct} = \nu_t/D_t$, for the wake-wall boundary layer flow were found to be 0.5 ± 0.2 (Kacker, Pai and Whitelaw, 1969). Since there is little justification for using a particular value or functional variation for S_{ct}, we take $S_{ct} = 0.7$ and $\nu/D = 1$ in the present investigation. The last integral in Eq. (4.16) now can be evaluated as

$$\int_{U_o}^{1} (\cdots) dU = \begin{cases} \int_{U_o}^{U_m} (\cdots) dU + \int_{U_m}^{1} (\cdots) dU & \text{if } U_m \geqslant U_o \\ \int_{U_o}^{1} (\cdots) dU & \text{if } U_m < U_o \end{cases}$$

where $(\cdots)$ represents symbolically the integrand, U_m is the value where the wall region meets the wake region and is determined by Eq. (2.28).

4.1.2 Initial Conditions

The location x_o is determined by $s = \delta_w + \delta_f$ (see Fig. 1).

Based on the nature of parabolic partial differential equations and the assumption for the mean velocity distribution at x_o, only the initial conditions and boundary conditions in the free stream and the wall are required and the mean velocity profile of the merged flow coincides with that of the superposition of both free mixing layer and wall boundary layer at x_o, the necessary initial values for $\{b_o, b_1, \ldots, b_{N-1}\}$ can be obtained by the following method. We consider the mean velocity and Z distributions at x_o as shown in Fig. 9. The singularity of Z within $0 < U < 1$ only exists at $x = x_o$ because the interaction between the free mixing layer and the wall layer causes a momentum change which will smooth the velocity profile, and hence the Z profile after x_o. Presumably, we may extrapolate the U and Z profiles as shown in the dashed line on the same figure, and therefore use the new profiles as initial conditions. This is possible because the estimate of the locations of the edges of the wall boundary layer and the free mixing layer is rough, say at $U = 0.98$ for the wall layer and $U = 0.1$ (note the definition of U for the mixing layer is different from that of the wall layer) for the lower edge of the free mixing layer. The method of obtaining initial values for $\{b_o, b_1, \ldots, b_{N-1}\}$ based on the new profile is the same as that described in Chapter 2. The initial value for U_o in Eq. (4.16) is simply equal to λ at $x = x_o$.

4.2 Results and Discussion

In this section, theoretical predictions, based on the approximation $N = 3$, for velocity profiles, skin friction coefficients and concentration profiles are presented and discussed; representative integral properties are also presented. The calculations were

carried out at three values of the velocity ratio U_2/U_1, namely 0.9, 0.7 and 0.51; and at one value of slot height, namely s = 1 cm. The flow conditions of the injected mass are fixed and identical to those given in Coles and Hirst (1968) for the case ID 1400.

The shapes of the mean velocity profiles along the streamwise direction are shown in Figs. 10, 11 and 12. It can be seen that there is a region in which the velocity gradient is increasing near the wall surface. This is due to the larger momentum of the upper stream which thins the sublayer of the wall boundary layer caused by the lower stream. Consequently, the local skin friction increases within this region. The corresponding concentration profiles of the upper stream are also shown in the same figures. The distribution of U_o, which is the parameter determining the concentration profile, is shown in Fig. 13. It may be noted that the larger the value of the velocity ratio, the greater is the distance to the location where the mass concentration diffuses to the wall surface. As indicated in Chapter 3, a smaller velocity ratio results in a larger mixing region; thus the merging between the mixing layer and the wall layer occurs over a shorter distance. Physically, the larger velocity ratio produces greater momentum in the upper stream and the lower stream is unable to sustain the greater impingement within the same distance.

It is interesting to examine the local skin friction distribution in Fig. 14. For velocity ratio $U_2/U_1 = 0.9$ and $U_2/U_1 = 0.7$, the local skin friction distributions first decrease and then increase over a short distance, finally decreasing in the streamwise direction. The first decrease exists because the lower stream can sustain the impingement of the upper stream over a short distance. The increase, as mentioned earlier, is due to the sublayer of the wall layer and

results from the lower stream being thinned by the impingement of the upper stream. The final decrease is due to the development of the flow in the conventional turbulent boundary layer. For the velocity ratio $U_2/U_1 = 0.51$, unlike the other cases, the skin friction increases and then decreases, owing to the fact that the lower stream can not sustain the impingement of the upper stream under such a velocity ratio.

Figures 15, 16 and 17 show the distributions of the integral properties, namely shape factor H, displacement thickness δ^* and momentum thickness θ. During the interaction process of the free mixing layer and the wall layer, the shape factor decreases due to the decrease in displacement thickness (recall that the sublayer next to the wall is thinned) and the increase in momentum thickness. Finally, the shape factor approaches a constant value which is equal to that for a conventional turbulent boundary layer over a flate plate with zero pressure gradient.

All arguments made above are physically reasonable; however, the predictions should be compared with experimental data. Unfortunately, to the author's knowledge, there is no such data corresponding to the type of flow considered here. It is therefore suggested that the experiments on such flow be conducted in the future.

V. CONCLUSION

A model for reducing the corrosive effects on a wall surface in a coal gasification process has been established. In this, a non-corrosive gas is injected beneath the main stream of the coal gas products in a direction parallel to the wall surface. The solution procedure consists of (1) solving the development of a turbulent wall boundary layer, (2) solving the development of a turbulent free mixing layer, and (3) solving the interaction between the wall layer and the mixing layer.

The application of the orthonormal version of the Method of Integral Relations (MIR) to the present investigation has been studied. As far as the development of the turbulent wall boundary layer is concerned, numerical results are shown to be in good agreement with experimental data. In addition, a means of determining the initial conditions from the experimental data at the initial station has been suggested and has proven to be effective. Regarding the development of the turbulent free mixing layer, MIR eliminates the velocity component v from the governing equations. The traditional third boundary condition does not appear in the present formulation. Numerical results are also shown to be in good agreement with the available experimental data.

Numerical results of the analysis for the interaction between the wall layer and the mixing layer are plausible. A new boundary layer type flow is found within the distance of the interaction. In this, the skin friction coefficient may increase or decrease firstly, depending on the ratio of the main stream speed to the

injected stream speed, then subsequently increases, and finally decreases along the streamwise direction. The interaction eventually leads to the formation of the conventional turbulent boundary layer.

Finally, the species equation is solved and the ratio of the distance protected from attack by the corrosive gas to the slot height is found to be of the order $O(100)$.

REFERENCES

Abbott, D. E., and Deiwert, G. S., "Application of the Method of Weighted Residuals to the Turbulent Boundary-Layer Equations," Proceedings, Computation of Turbulent Boundary Layers – 1968 AOFSR-IFP-Stanford Conference, Vol. 1 (1968), pp. 46-53.

Birch, S. F., and Eggers, J. M., "A Critical Review of the Experimental Data for Developed Free Turbulent Shear Layers," NASA Langley Working Conference on Free Turbulent Shear Flows (1972).

Bradshaw, P. (ed.), Topics in Applied Physics-Turbulence, Vol. 12, Springer-Verlag (1976).

Brown, G. L., and Roshko, A., "On Density Effects and Large Structure in Turbulence Mixing Layers," J. Fluid Mech., 64 (1974), pp. 775-816.

Brune, G. W., "Theoretical Prediction of Confluent Boundary Layers," Third Symposium on Turbulent Shear Flows, University of California, Davis (1981), pp. 1.21-1.27.

Cary, A. M., Bushnell, D. M., and Hefner, J. N., "Predicted Effects of Tangential Slot Injection on Turbulent Boundary Layer Flow over a Wide Speed Range," ASME, J. of Heat Transfer, Vol. 101 (1979), pp. 699-704.

Clauser, F. H., "The Turbulent Boundary Layer," Advances in Applied Mechanics, Vol. 4 (1956), pp. 1-51.

Coles, P., and Hirst, E. (eds.), Proceedings, Computation of Turbulent Boundary Layers – 1968 AFOSR-IFP Stanford Conference, Vol. 2, Compiled Data (1968).

Dvorak, F. A., "Calculation of Turbulent Boundary Layers and Wall Jets over Curved Surfaces," AIAA Journal, Vol. 11, No. 4 (1973), pp. 517-524.

Dorodnitsyn, A. A., "General Method of Integral Relations and Its Application to Boundary Layer Theory," Advances in Aeronautical Science, Vol. 3, Pergamon Press, New York (1960).

Fletcher, C. A. J., and Holt, M., "An Improvement of the Method of Integral Relations," J. of Computational Physics, Vol. 18, No. 2 (1975), pp. 154-164.

Görtler, H., "Berechnung von Aufgaben der freien Turbulenz auf Grund eines neuen Näherungsansatzes," ZAMM, 22 (1942).

Isaacson, E., and Keller, H. B., Analysis of Numerical Methods, 1st ed., Wiley, New York (1966), p. 199.

Kacker, S. C., Pai, B. R., and Whitelaw, J. H., "The Prediction of Wall Jet Flows with Particular Reference to Film Cooling," Progress in Heat and Mass Transfer, Vol. 2, Pergamon Press, Inc. (1969), pp. 163-186.

Kleinstein, G., "Generalized Law of the Wall and Eddy-Viscosity Model for Wall Boundary Layers," AIAA Journal, Vol. 5, No. 8 (1967), pp. 1402-1407.

Kuethe, A. M., "Investigation of the Turbulent Mixing Regions Forced by Jets," ASME, J. of Applied Mechanics, Vol. 2 (1935), pp. A87-95.

LaRue, J. C., and Libby, P. A., "Measurements in the Turbulent Boundary Layer with Slot Injection of Helium," Phys. of Fluids, Vol. 20, No. 2 (1977), pp. 192-202.

LaRue, J. C., and Libby, P. A., "Further Results Related to the Turbulent Boundary Layer with Slot Injection of Helium," Phys. of Fluids, Vol. 23, No. 6 (1980), pp. 1111-1118.

Mills, R. D., "Numerical and Experimental Investigations of the Shear Layer Between Two Parallel Streams," J. of Fluid Mechanics, Vol. 33 (1968), pp. 591-616.

Miner, E. W., and Lewis, C. H., "Numerical Studies of Supersonic Turbulent Boundary-Layer Flows with Tangential Slot Injection," Computer Methods in Applied Mechanics and Engineering, Vol. 4 (1974), pp. 19-38.

Murphy, J. D., and Rose, W. C., "Application of the Method of Integral Relations to the Calculation of Incompressible Turbulent Boundary Layers," Proceedings, Computation of Turbulent Boundary Layers — 1968 AFOSR-IFP-Stanford Conference, Vol. 1 (1968), pp. 54-75.

Pot, P. J., "A Wake Boundary Layer Mixing Experiment," Second Symposium on Turbulent Shear Flows, Imperial College (1979), pp. 6.6-6.11.

Prandtl, L, "Bemerkungen zur Theorie der freien Turbulenz," ZAMM, Vol. 22 (1942), pp. 241-243.

Rodi, W., "A Review of Experimental Data of Uniform Density Free Turbulent Boundary Layers," Studies in Convection, Vol. 1, Ed. B. E. Launder, Academic Press (1975).

Seban, R. A., and Back, L. H., "Velocity and Temperature Profiles in Turbulent Boundary Layers with Tangential Injection," ASME, J. of Heat Transfer, Vol. 84 (1962), pp. 45-54.

Spalding, D. B., "A Single Formula for the Law of the Wall," ASME, J. of Applied Mechanics, Vol. 28 (1961), pp. 455-457.

Ting, L., "On the Mixing of Two Parallel Streams," J. of Math. and Phys., Vol. 38, 153 (1959), pp. 153-165.

Tollmien, W., "Berechnung turbulenter Ausbreitungsvorgänge," ZAMM, Vol. 6 (1926), p. 6.

Townsend, A. A., "The Structure of Turbulent Shear Flow," Cambridge University Press (1976).

Yeung, W. S., and Yang, R. J., "Application of the Method of Integral Relations to the Calculation of Two-Dimensional Incompressible Turbulent Boundary Layer," ASME, J. of Applied Mechanics, Vol. 48 (1981), pp. 701-706.

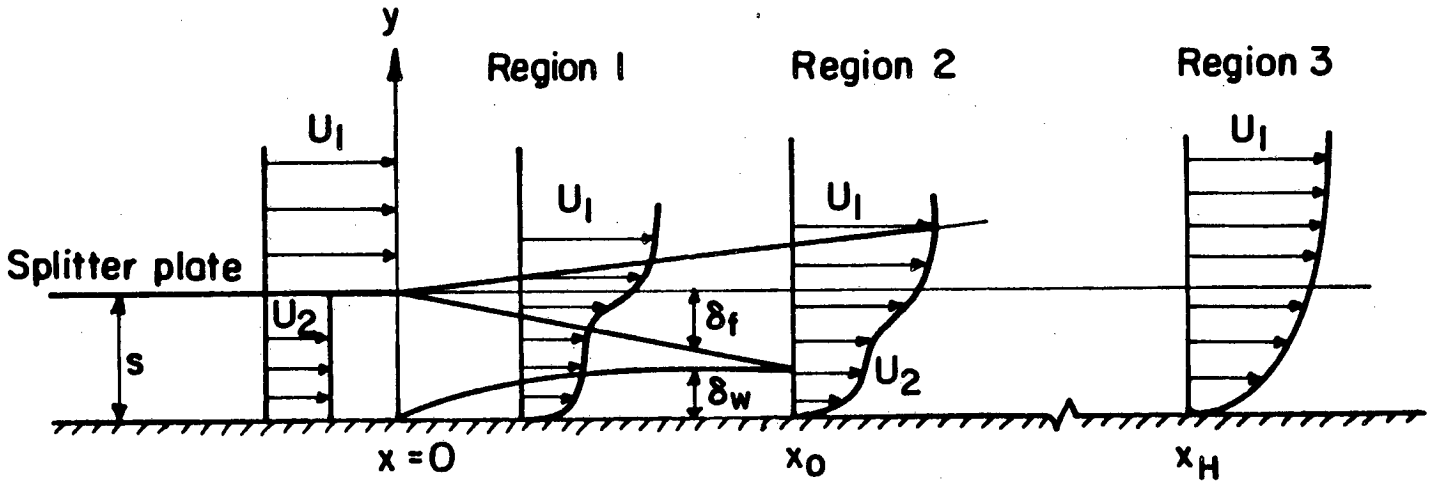

(a) Mean Velocity Profile

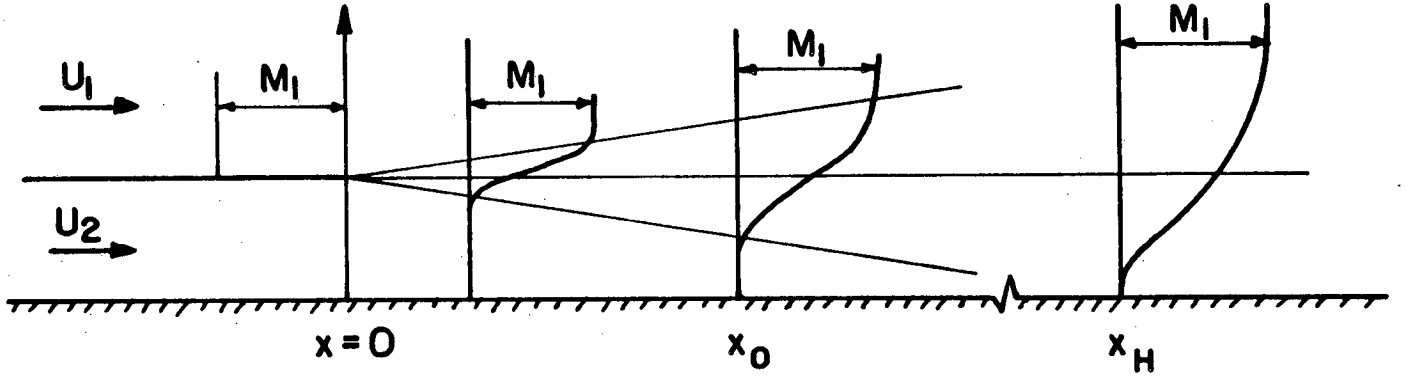

(b) Mean Mass Concentration Profile

XBL822-5183

Fig. 1 Illustration of velocity and concentration profiles for a tangential injection flow field.

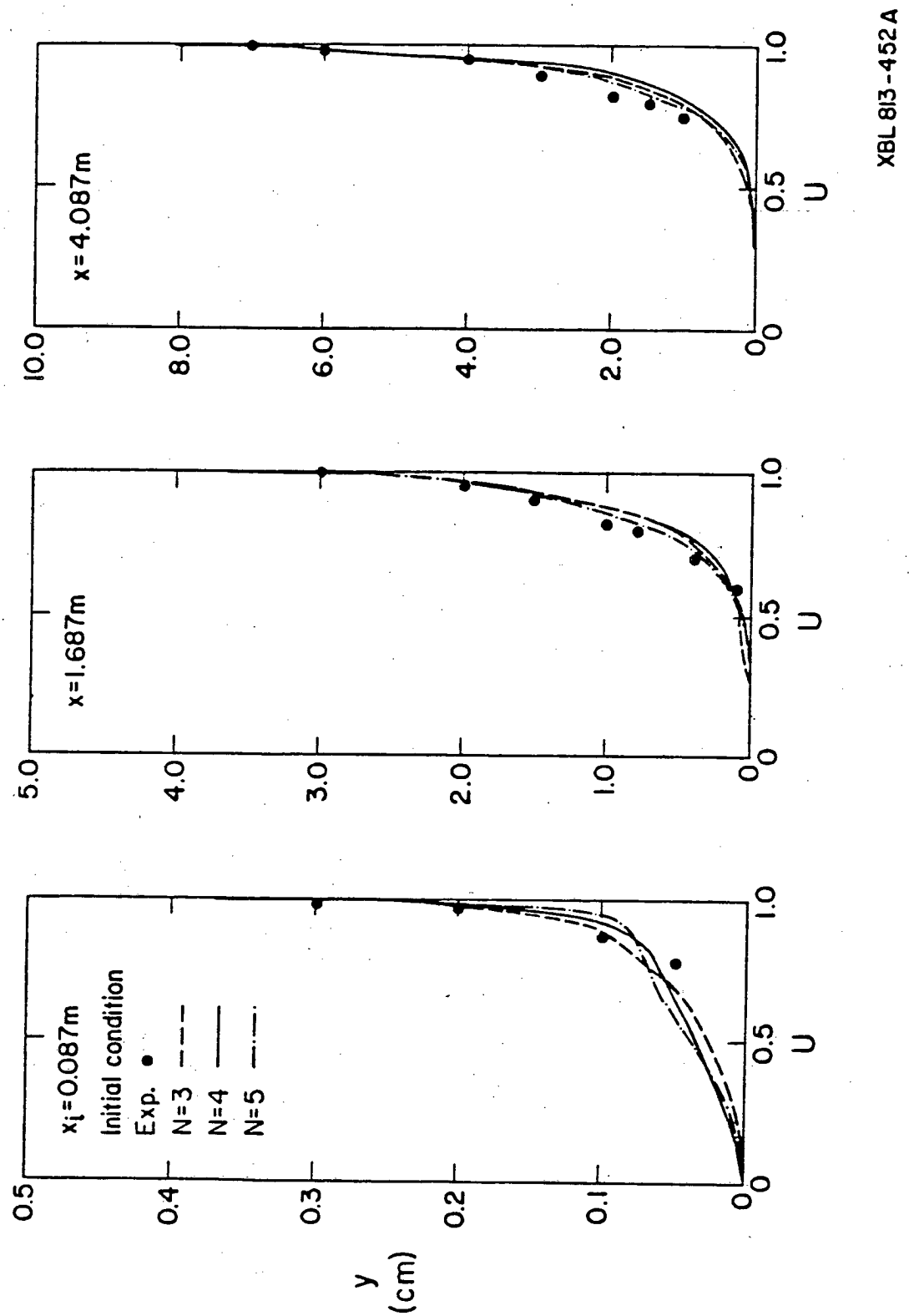

Fig. 2 Initial velocity profile and its development (ID 1400). (This and subsequent ID numbers are from Coles and Hirst, 1968).

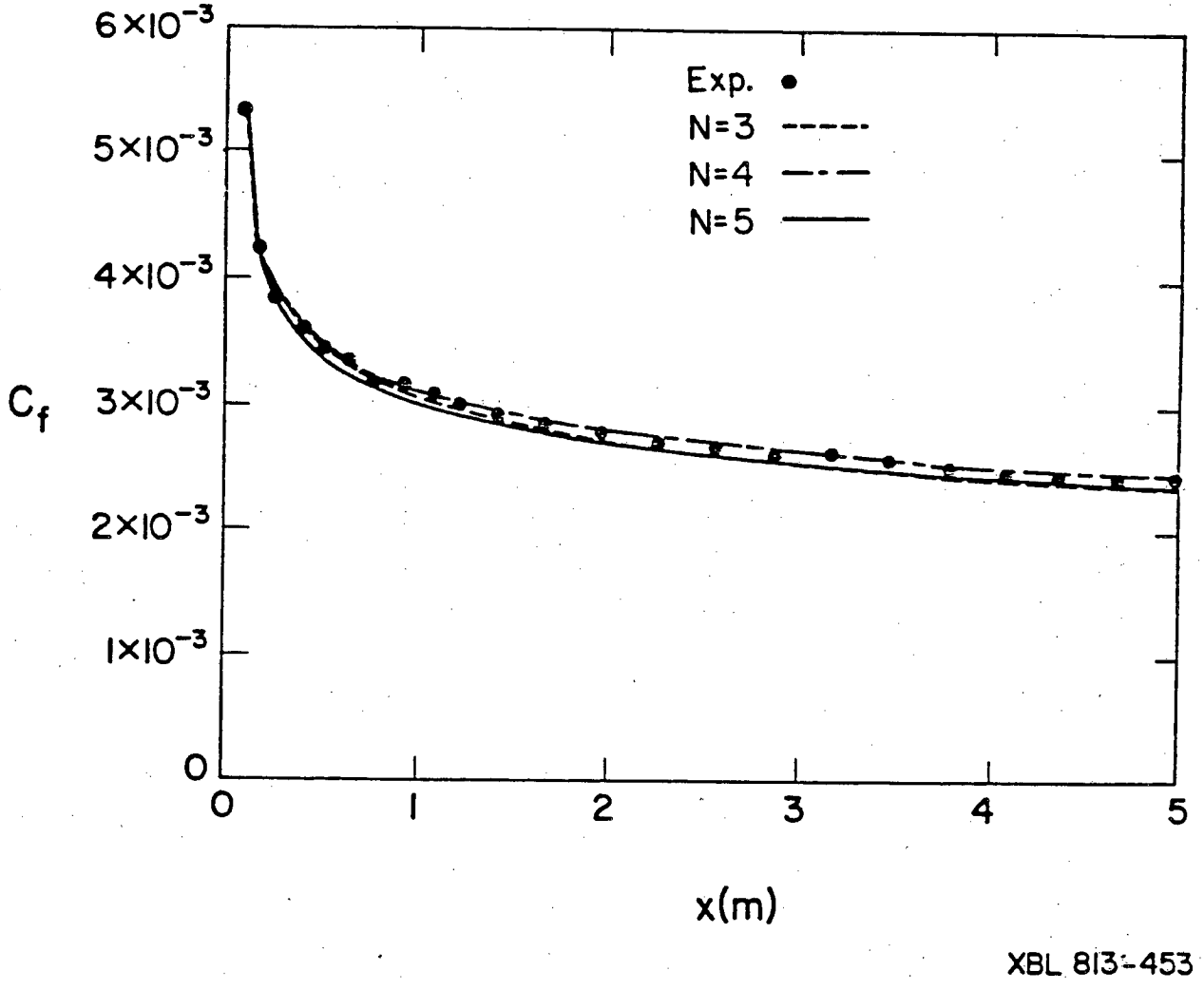

Fig. 3 Skin friction coefficient (ID 1400).

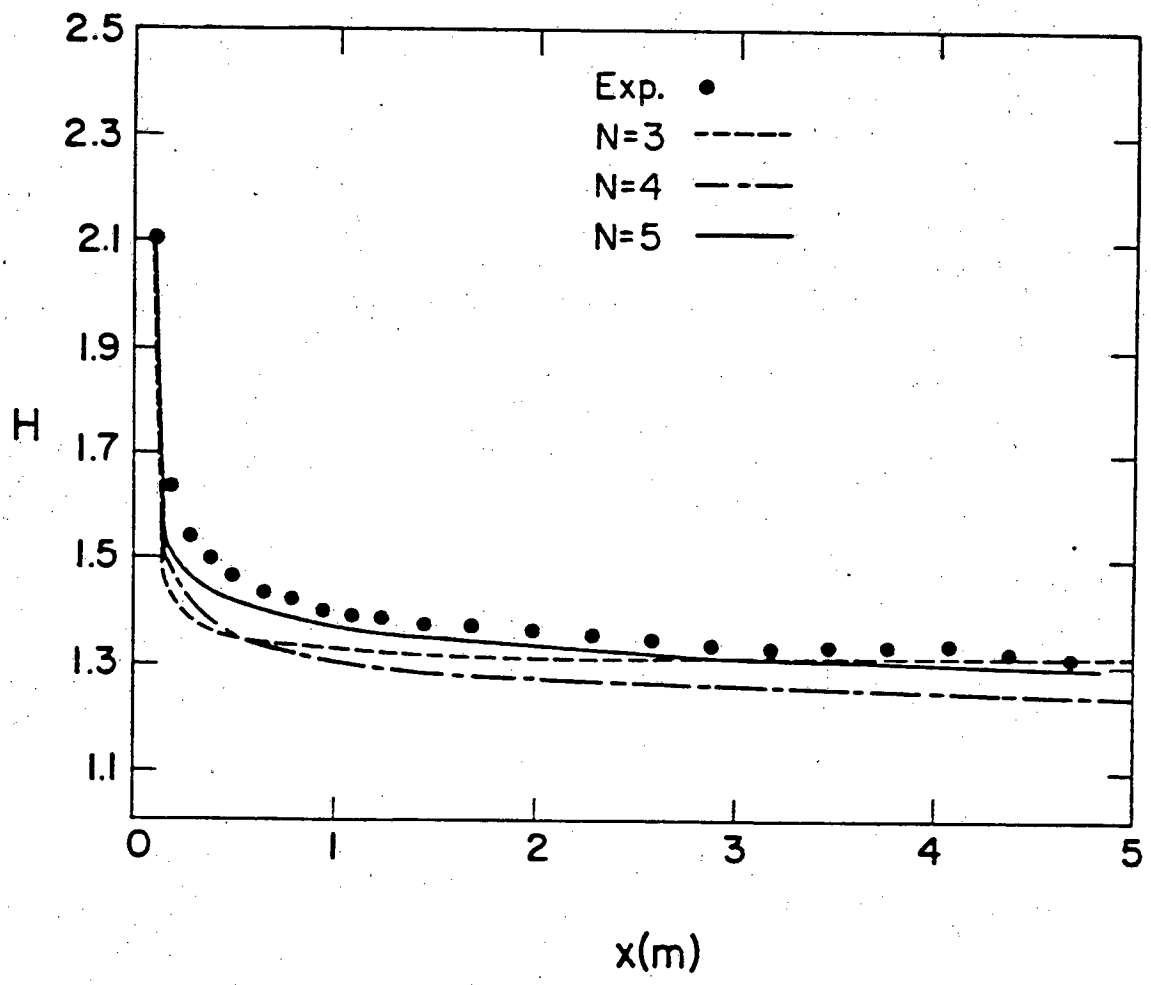

Fig. 4 Shape factor (ID 1400)

XBL 813-444

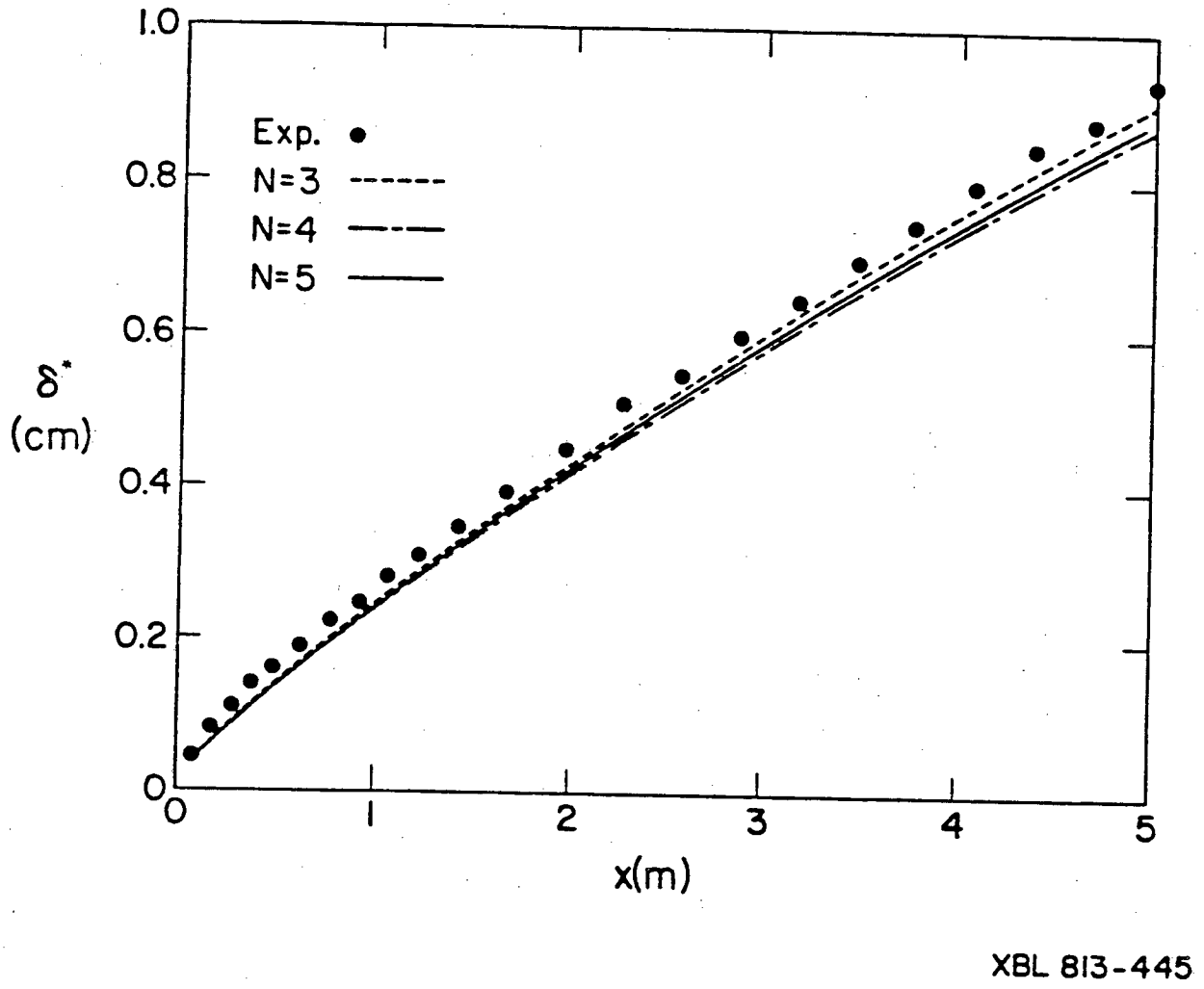

Fig. 5 Displacement thickness (ID 1400)

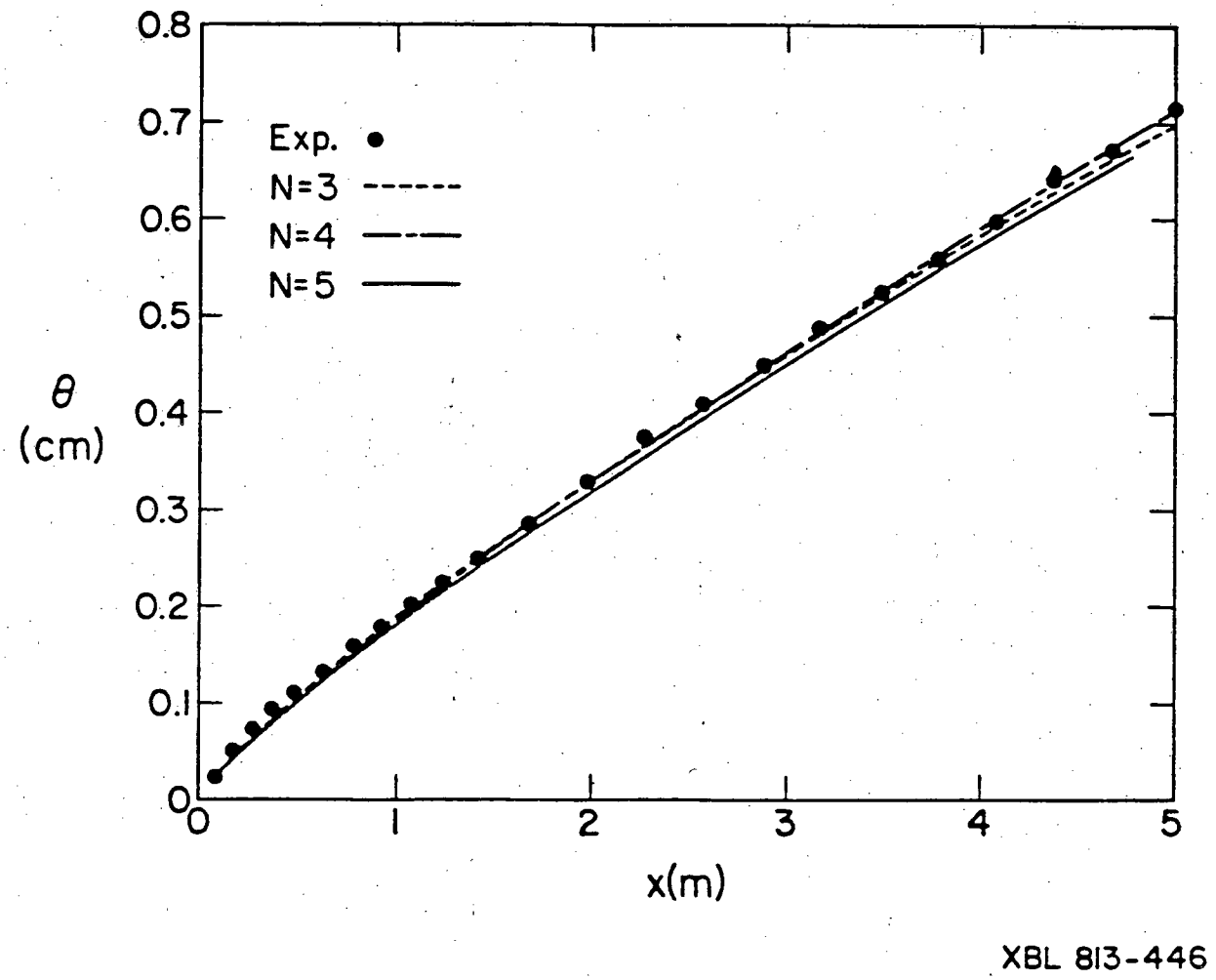

Fig. 6 Momentum thickness (ID 1400)

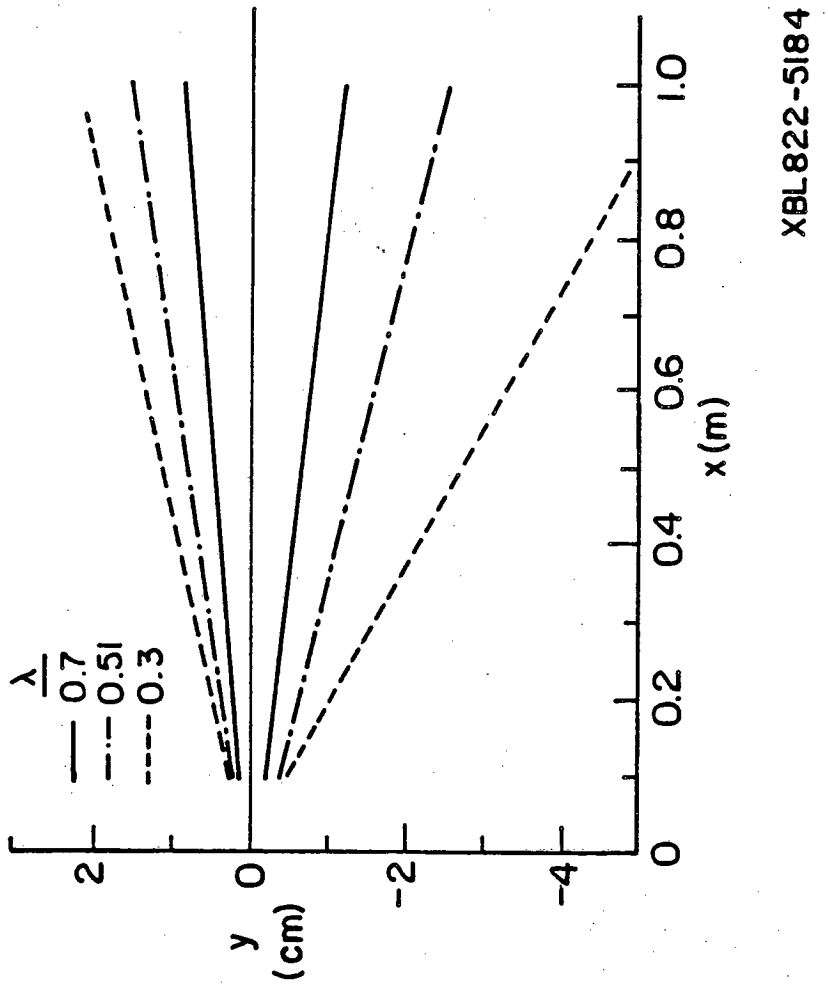

Fig. 7 Lines of constant velocity in the mixing region

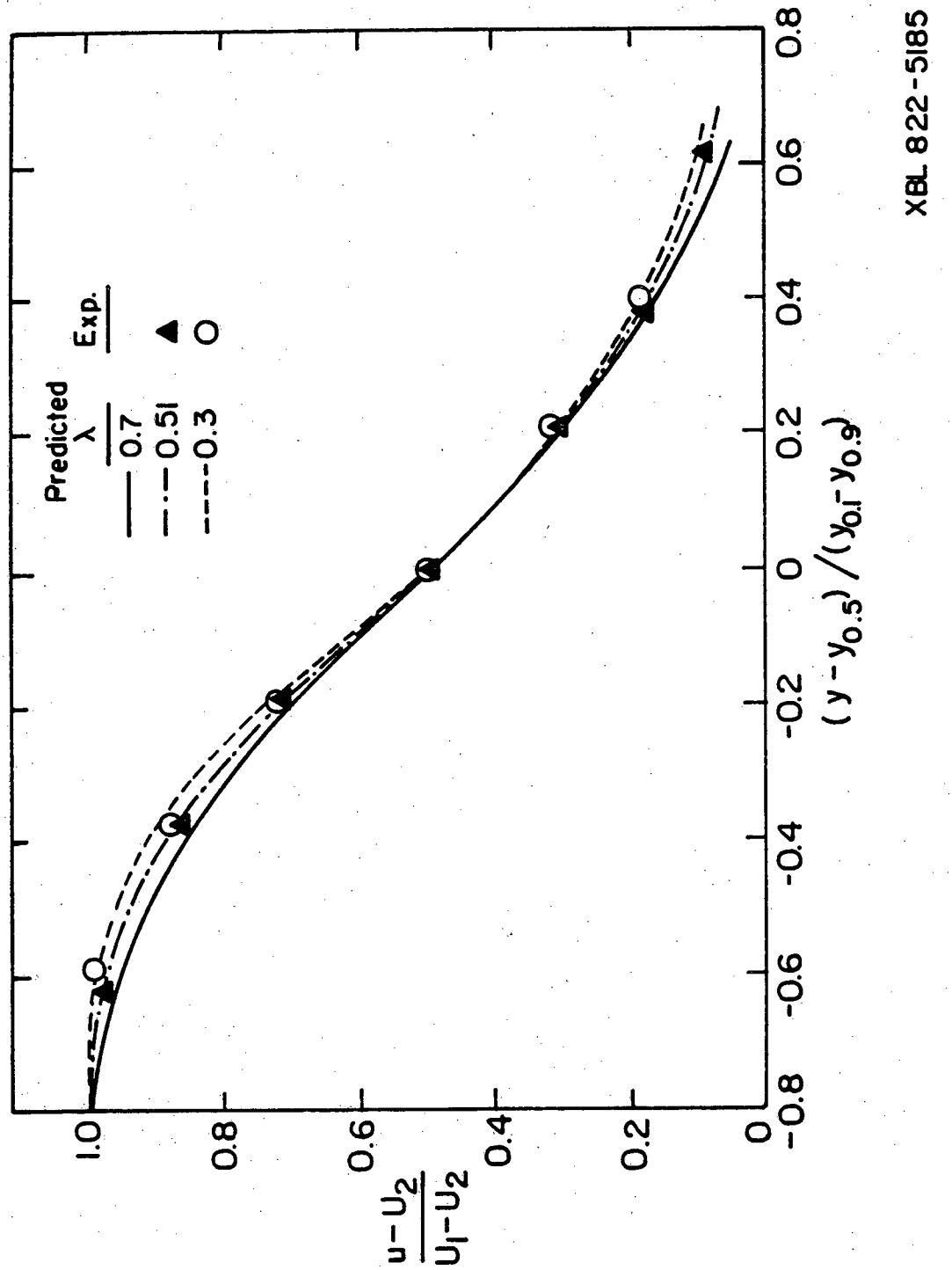

Fig. 8 Velocity distribution in the mixing region

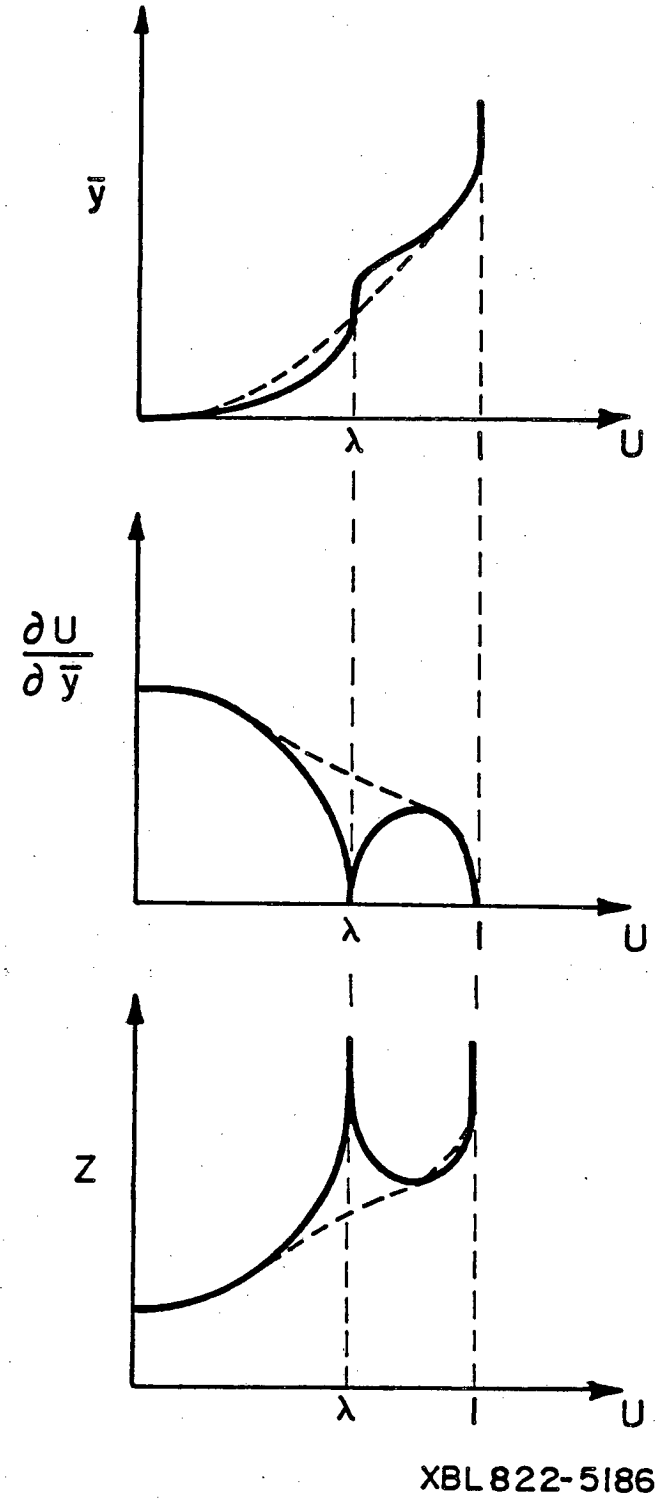

Fig. 9 Velocity and Z profiles at x_o.

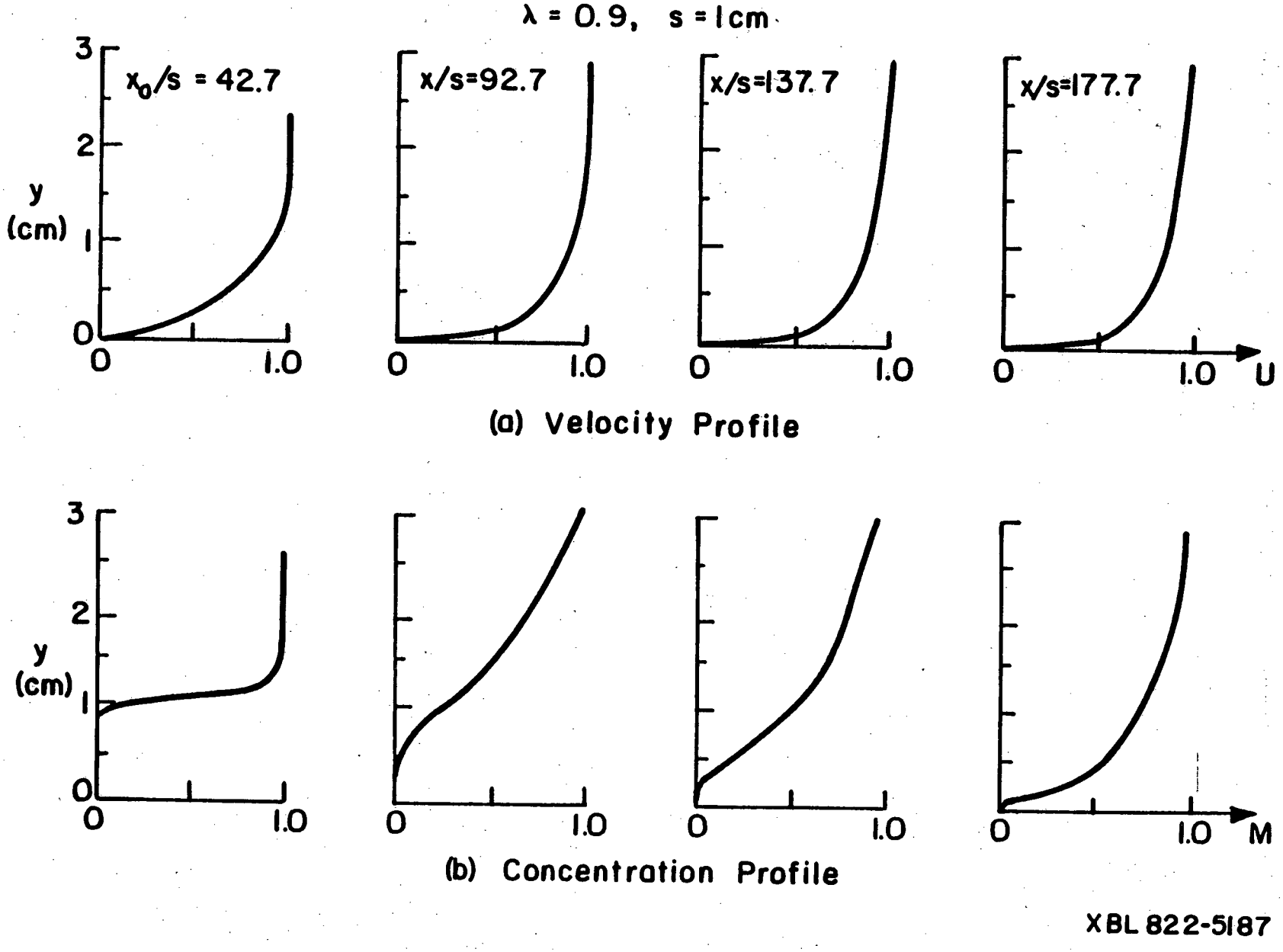

Fig. 10 The development of velocity profile and concentration profile in the streamwise direction

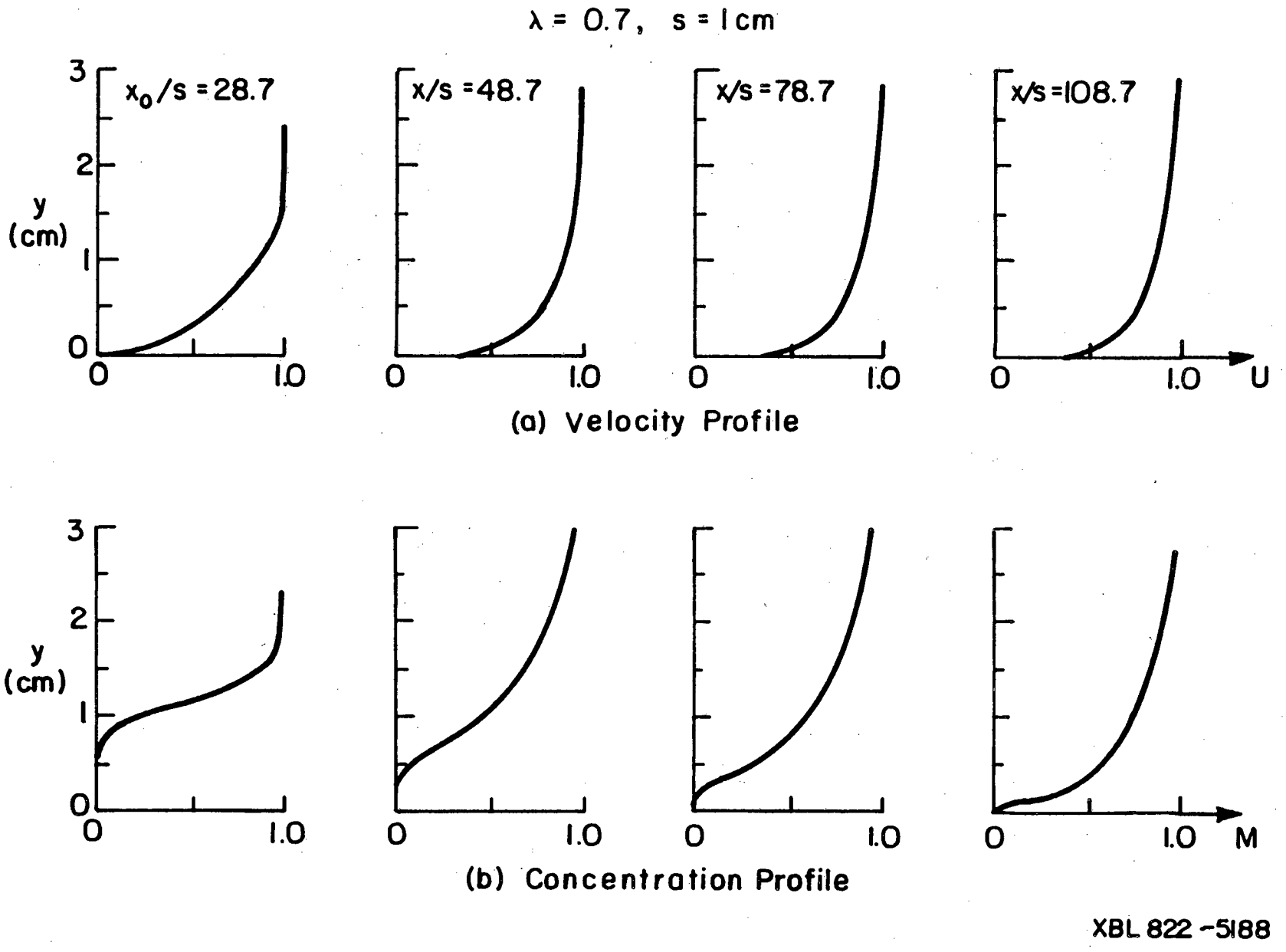

Fig. 11 The development of velocity profile and concentration profile in the streamwise direction

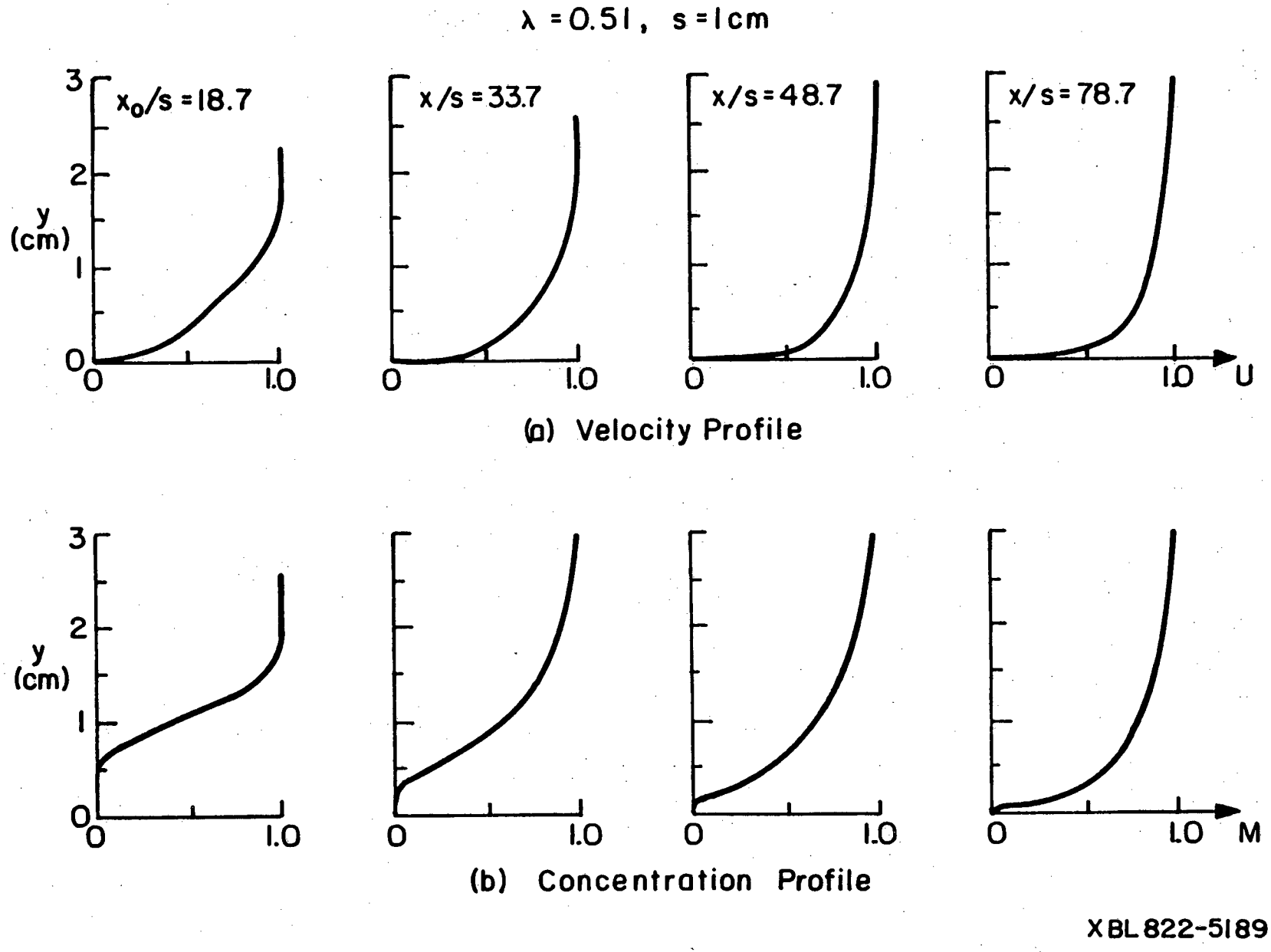

Fig. 12 The development of velocity profile and concentration profile in the streamwise direction

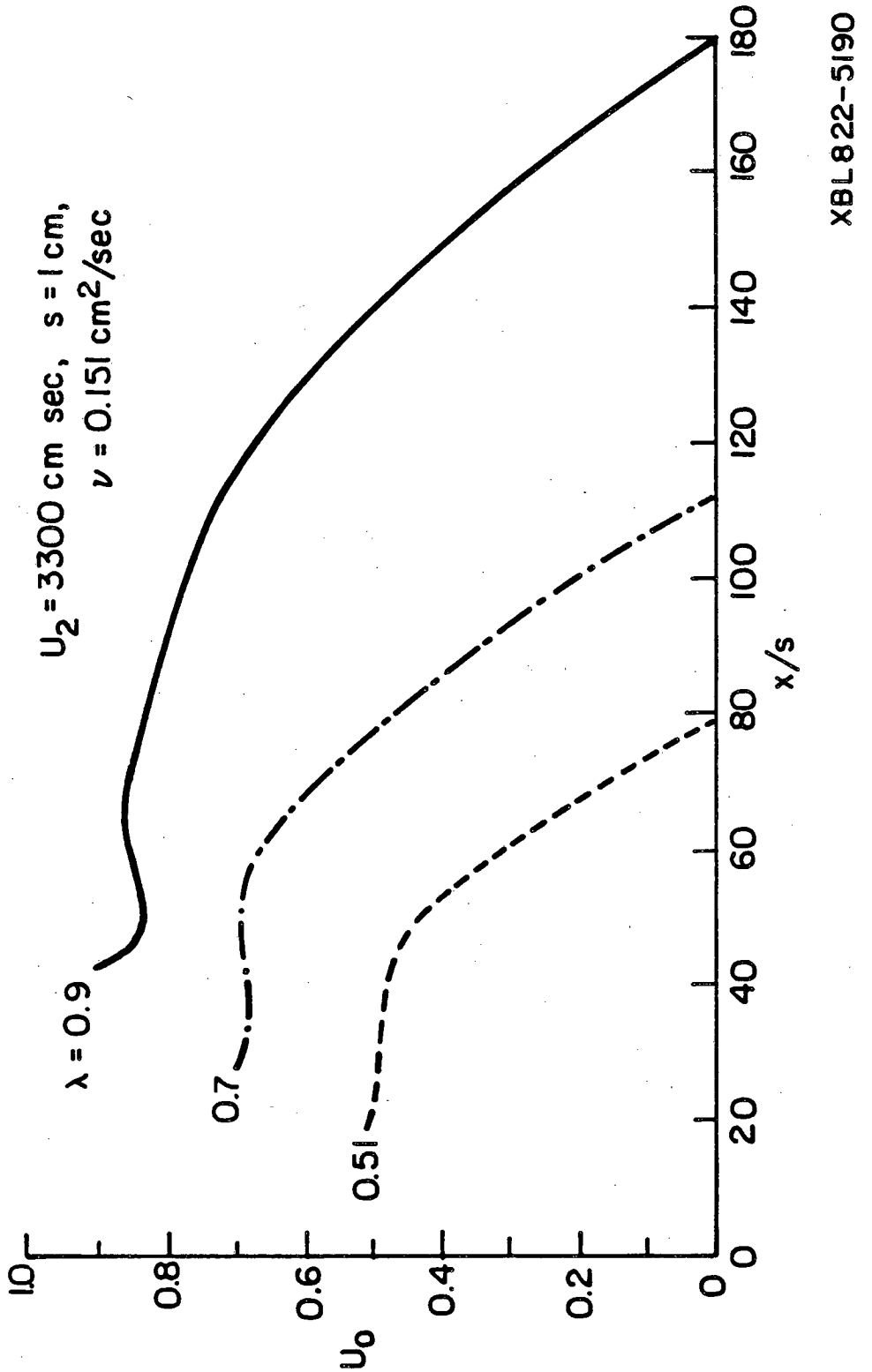

Fig. 13 Distribution of U_o

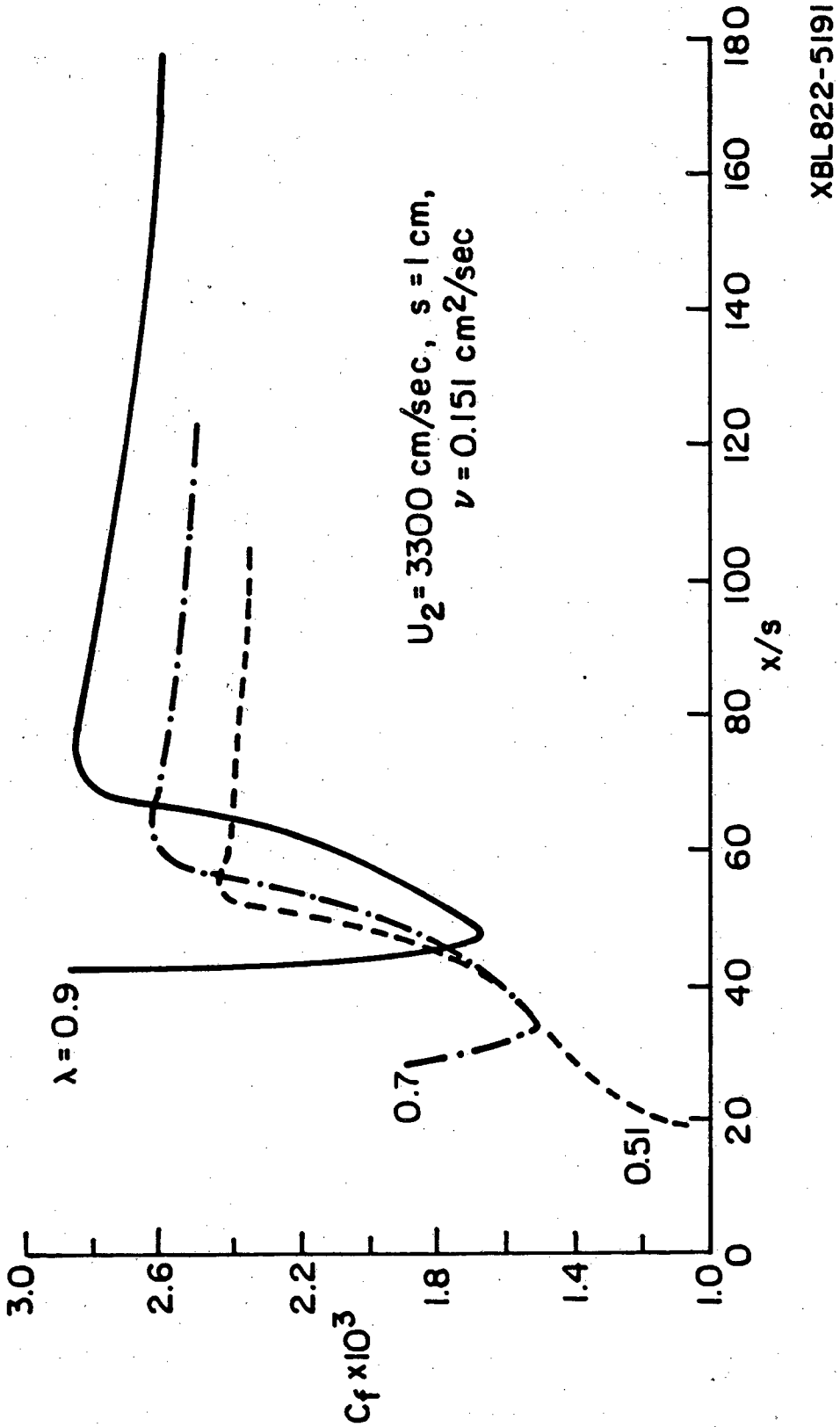

Fig. 14 Skin friction coefficient

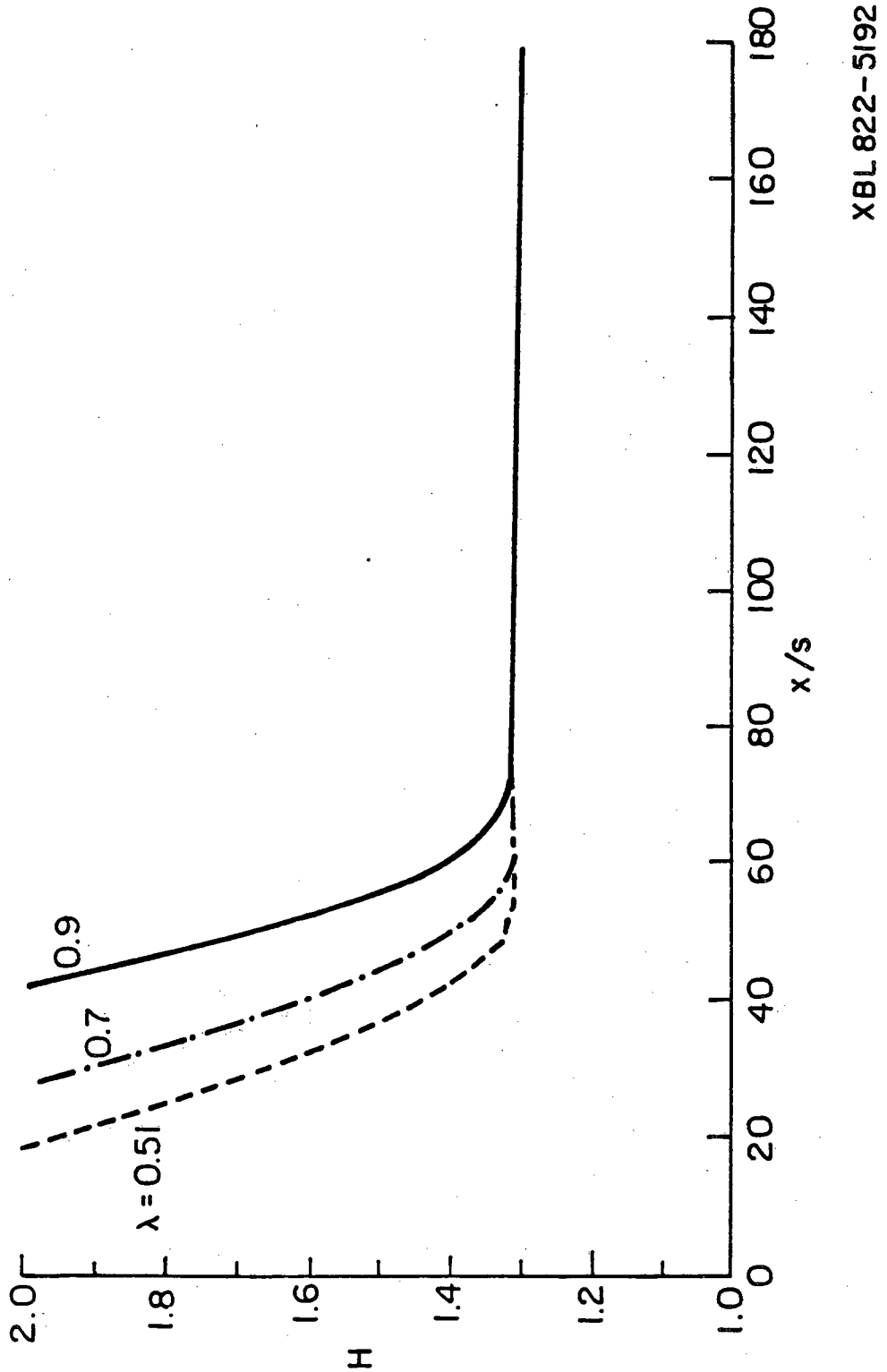

Fig. 15 Shape factor

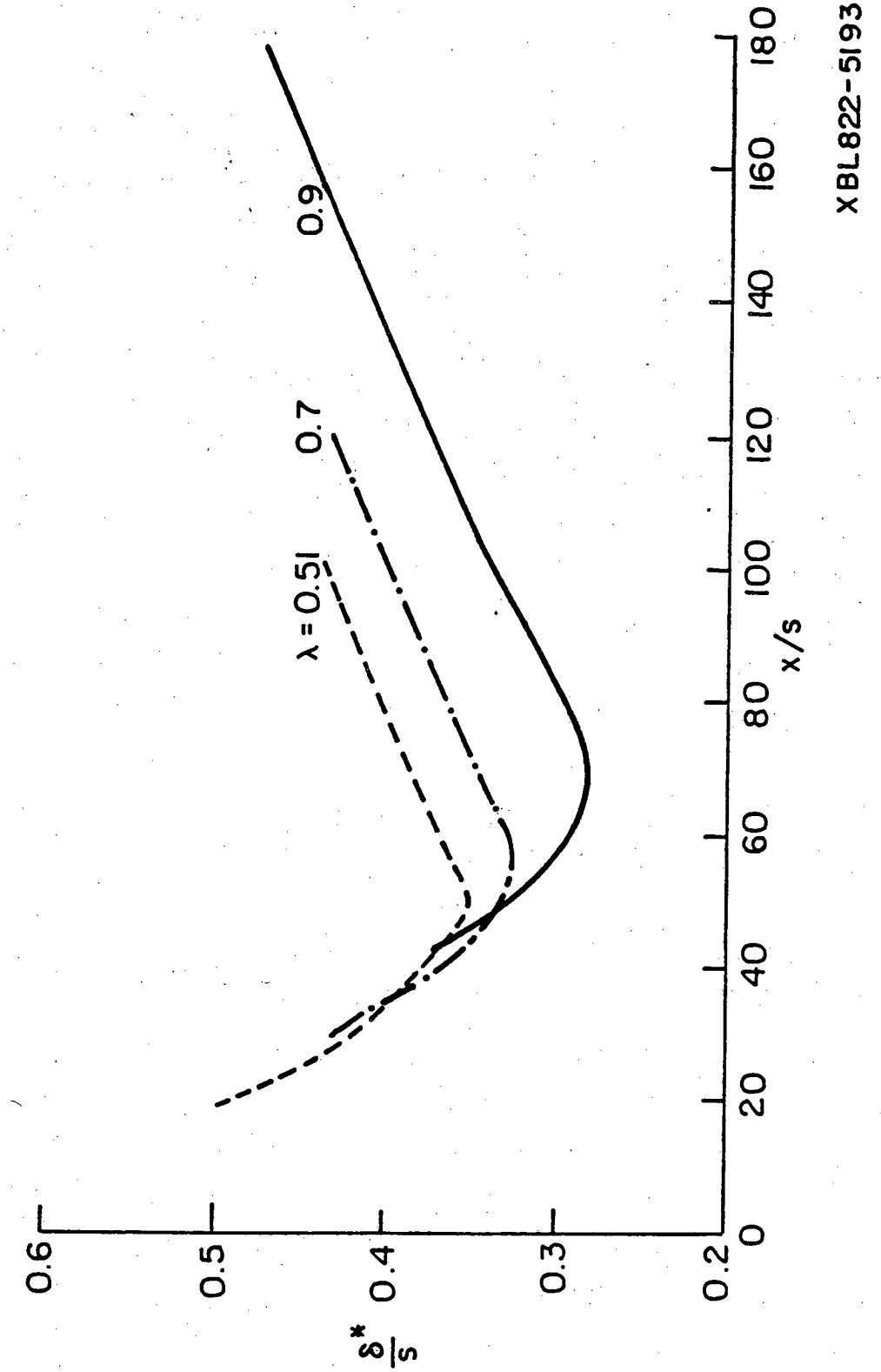

Fig. 16 Displacement thickness

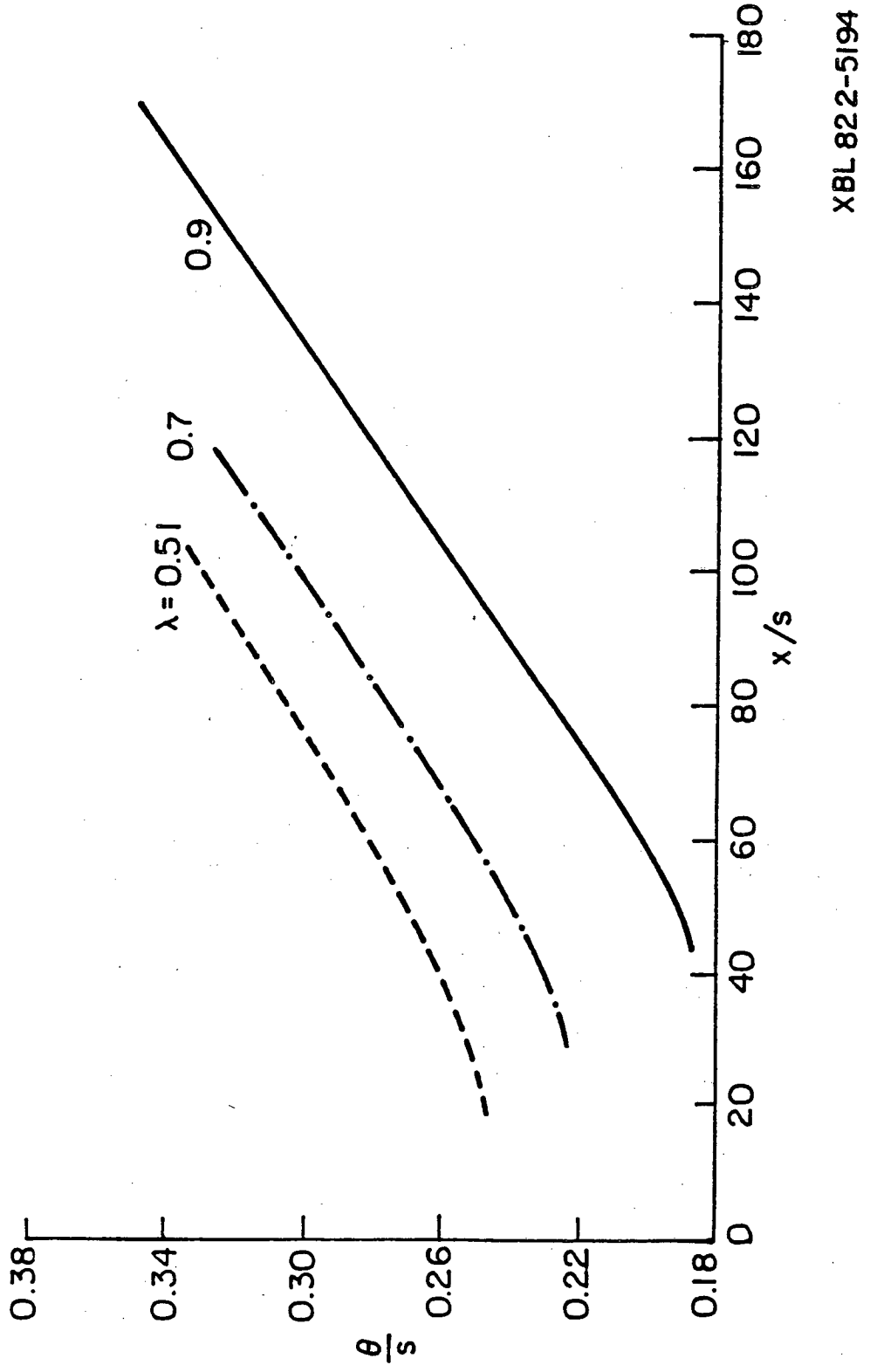

Fig. 17 Momentum thickness

TECHNICAL INFORMATION DEPARTMENT
LAWRENCE BERKELEY LABORATORY
UNIVERSITY OF CALIFORNIA
BERKELEY, CALIFORNIA 94720